LUND
UNIVERSITY

Top Threshold Revisited

Torbjörn Sjöstrand

Department of Physics, Lund University

with input from **Valery Khoze**, Durham University
and **Christian Preuss**, University of Göttingen

Toponium Day, CERN, 14 January 2026

Pseudo-bound "toponium" revival

CMS Collaboration, Rept.Prog.Phys. 88 (2025) 8, 087801 (2503.22382 [hep-ex])

$\sigma(\eta_t) = 8.8 \pm^{+1.2}_{-1.4}$ pb.

Require: ℓ^+, ℓ^-, two b tags, solve for two ν, mass cuts.

Study: $c_{\rm hel} = \hat{\ell}^+_t \cdot \hat{\ell}^-_{\bar{t}}$ + more

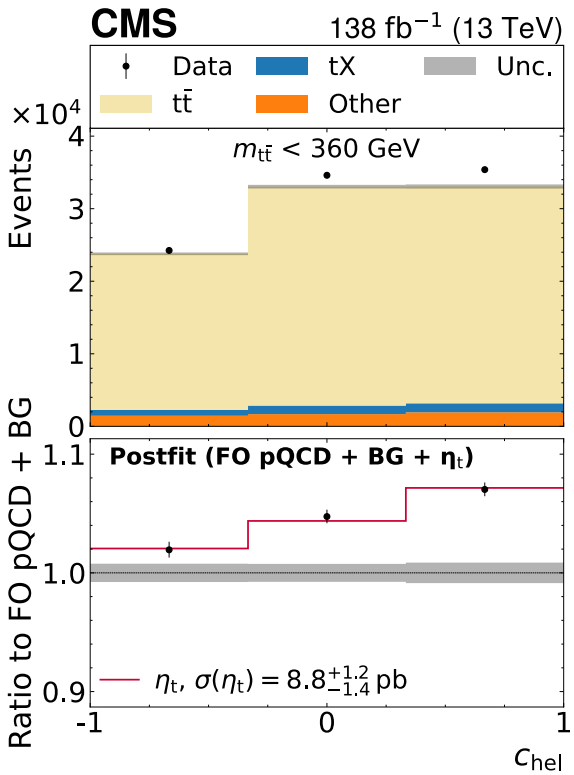

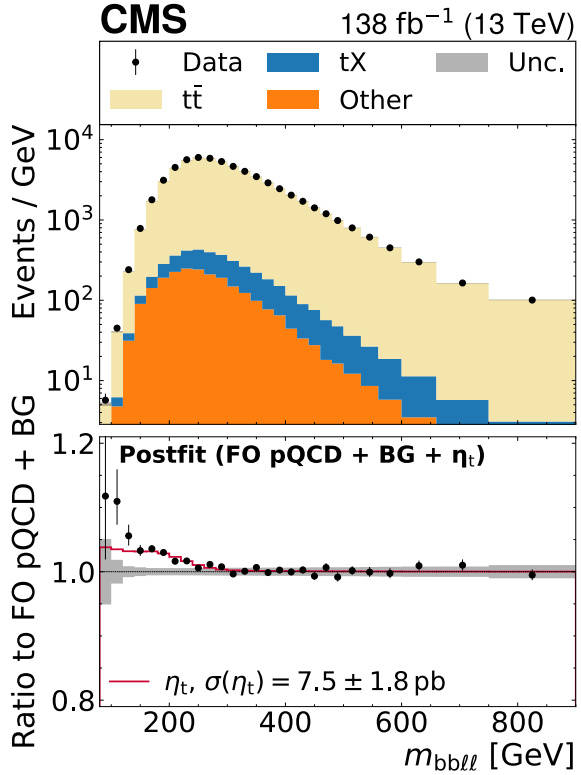

ATLAS-CONF-2025-008, similar approach,

$\sigma_{\rm excess} = 9.0 \pm 1.3$ pb.

Prehistory: the third generation

1973 CPV with 3 quark generations, M. Kobayashi and T. Maskawa

1975 τ lepton, SPEAR at SLAC, M.L. Perl et al.

1977 Υ, E288 at Fermilab, L. Lederman et al.

1978 $\Upsilon \to \mathrm{ggg}$, PLUTO at DESY

1978 (ca) "most" theorists expect $m_{\mathrm{t}} \approx 15$ GeV since

$$\frac{m_{\mathrm{c}}}{m_{\mathrm{s}}} \approx \frac{1.6}{0.5} \approx 3 \quad , \quad \frac{m_{\mathrm{b}}}{m_{\mathrm{c}}} \approx \frac{5.0}{1.6} \approx 3 \quad \Rightarrow \quad \frac{m_{\mathrm{t}}}{m_{\mathrm{b}}} \approx \frac{15.0}{5.0} \approx 3$$

with narrow $\mathrm{t\bar{t}}$ bound state decaying to ggg (and γ^*)

1979 – top exclusion gradually shifts upwards, notably PETRA at DESY

1984 UA1 at CERN finds top at $m_{\mathrm{t}} \approx 40$ GeV

1987 $\mathrm{B}^0 - \overline{\mathrm{B}}^0$ oscillations at ARGUS at DESY implies massive top; notably toponium (if any) mainly decaying weakly

1994 top evidence by CDF at Fermilab; **1995** discovery by CDF and D0

Early top threshold studies – 1

I. Bigi, Y. Dokshitzer, V. Khoze, J Kühn, and P. Zerwas,
Phys. Lett. 181B (**1986**) 157:
$m_{\mathrm{t}} > 125$ GeV $\Rightarrow t_{\mathrm{decay}} < t_{\mathrm{revolution}}$ for $\mathrm{t\bar{t}}$ state, and yet e.g.

$$\sigma(\mathrm{pp/p\bar{p}} \to 0^{-+}_{\mathrm{t\bar{t}}} + X) \sim \frac{\pi^2}{8m^2_{\mathrm{t\bar{t}}}} \frac{\Gamma(0^{-+}_{\mathrm{t\bar{t}}} \to \mathrm{gg})}{m_{\mathrm{t\bar{t}}}} \left[\tau \frac{\mathrm{d}\mathcal{L}}{\mathrm{d}\tau}\right]_{\mathrm{gg}}$$

V.S. Fadin and V.A. Khoze,
JETP Lett. 46 (**1987**) 417
(+ Yad. Fiz. 48 (**1988**) 487):
Green's function approach for
$\mathrm{e^+e^-} \to \gamma^*/\mathrm{Z}^0 \to \mathrm{t\bar{t}}$ threshold.

Figure: $m_{\mathrm{t}} = 140$ GeV,
dash-dotted Born, solid $\alpha_{\mathrm{s}} = 0.150$,
dashed $\alpha_{\mathrm{s}}(Q^2 = m_{\mathrm{t}}\sqrt{E^2 + \Gamma_{\mathrm{t}}^2})$

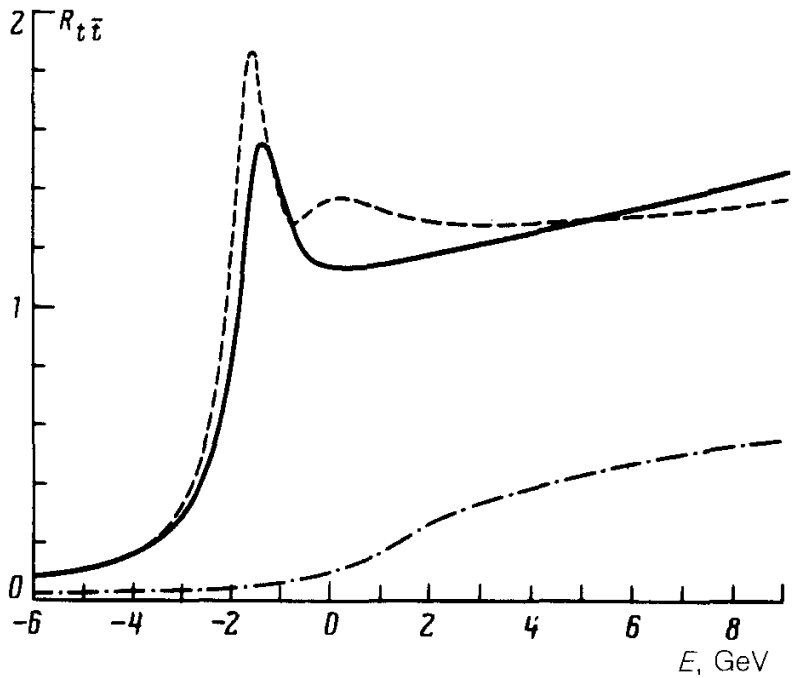

Early top threshold studies – 2

P. Nason, S. Dawson, R.K. Ellis,
Nucl.Phys.B 303 (**1988**) 607:
NLO calculation of
heavy flavour production;
note threshold enhancement
(and $m_{\rm t} = 40$ GeV)

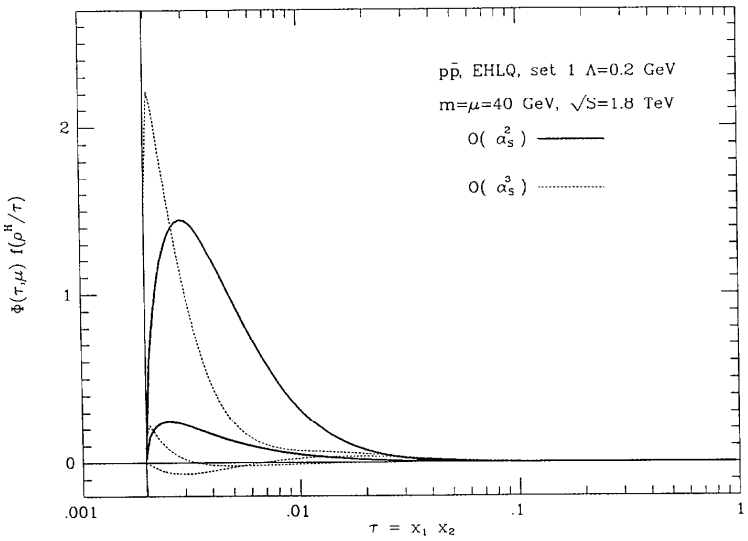

First (?) detailed studies of top threshold in $\rm pp/p\overline{p}$,
including pseudoscalar "toponium" contribution:
V.S. Fadin, V.A. Khoze, TS,
proceedings Moriond **1989**, Z. Phys. C48 (**1990**) 613,
(+ V.S. Fadin, V.A. Khoze, Sov.J.Nucl.Phys. 53 (**1991**) 692).
Unfortunately for $m_{\rm t} = 100$, 140 or 200 GeV, so update needed.

Since then many other studies, quite likely more sophisticated,
see further presentations today.

Kinematics and colour factors

$m_{\mathrm{t}} \approx 172.5$ GeV on-shell mass,
$\Gamma_{\mathrm{t}} \approx 1.34$ GeV Breit-Wigner width,
$m_{\mathrm{t}1}$ and $m_{\mathrm{t}2}$ Breit–Wigner-smeared t and $\bar{\mathrm{t}}$ masses,

$$\beta_{\mathrm{t}} = \sqrt{\left(1 - \frac{m_{\mathrm{t}1}^2}{\hat{s}} - \frac{m_{\mathrm{t}2}^2}{\hat{s}}\right)^2 - 4\,\frac{m_{\mathrm{t}1}^2}{\hat{s}}\,\frac{m_{\mathrm{t}2}^2}{\hat{s}}} = \sqrt{1 - 4\,\frac{\overline{m}_{\mathrm{t}}^2}{\hat{s}}}$$

which defines the "average" mass $\overline{m}_{\mathrm{t}}$ to preserve $|\mathbf{p}|$ in the $\mathrm{t}\bar{\mathrm{t}}$ rest frame.

Colour factors for $\mathrm{gg} \to \mathrm{t}\bar{\mathrm{t}}$:

$$\frac{\text{octet}}{\text{singlet}} = \frac{(d^{abc}/\sqrt{2})^2}{(\delta^{ab}/\sqrt{3})^2} = \frac{5}{2}$$

i.e. $\mathrm{gg} \to \mathrm{t}\bar{\mathrm{t}}$ is 2/7 singlet and 5/7 octet, while $\mathrm{q}\bar{\mathrm{q}} \to \mathrm{t}\bar{\mathrm{t}}$ is all octet.
Higher-order processes like $\mathrm{gg}/\mathrm{q}\bar{\mathrm{q}} \to \mathrm{gt}\bar{\mathrm{t}}$ could enhance singlet fraction, and switch from pseudoscalar 0^{-+} to vector 1^{--}.

Coulomb enhancement

QCD analogue of QED Sommerfeld, Gamow, Sakharov, ...

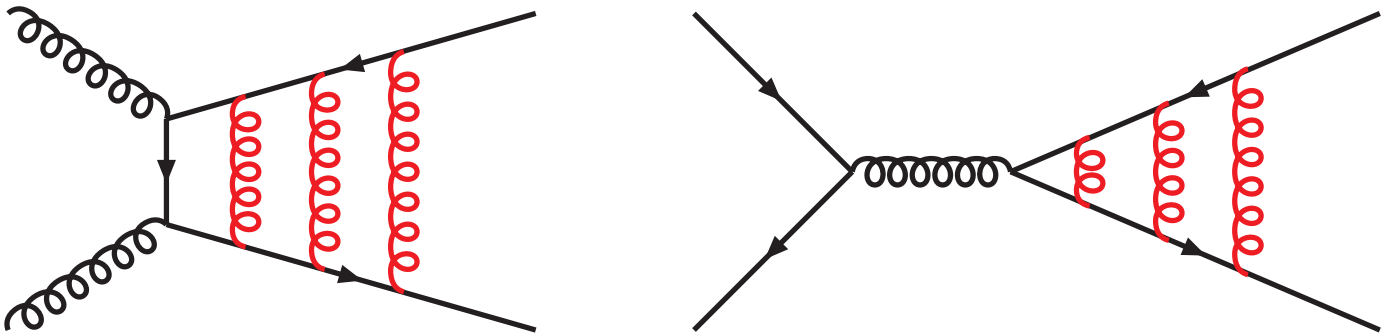

All-orders resummation of gluon exchange gives

$$|\psi^{(s)}(0)|^2 = \frac{X_{(s)}}{1-\exp(-X_{(s)})} \quad \text{with} \quad X_{(s)} = \frac{4}{3}\frac{\pi\alpha_s}{\beta_t} \ ,$$

$$|\psi^{(8)}(0)|^2 = \frac{X_{(8)}}{\exp(X_{(8)})-1} \quad \text{with} \quad X_{(8)} = \frac{1}{6}\frac{\pi\alpha_s}{\beta_t} \ ,$$

$$\alpha_s = \alpha_s\left(m_t\sqrt{E^2+\Gamma_t^2}\right) \ ,$$

$$E = \sqrt{\hat{s}} - 2m_t = \hat{m} - m_{t1} - m_{t2}$$

NRQCD Green's function (Fadin & Khoze)

$$\tilde{G}^{(s)}(E) = \frac{4\pi}{m_t^2}\Im G^{(s)}_{E+i\Gamma_t}(0,0) = \frac{p_2}{m_t} + \frac{2p_s}{m_t}\arctan\frac{p_2}{p_1} + \frac{2p_s^2}{m_t^2}\sum_{n=1}^{\infty}\frac{1}{n^4}\frac{\Gamma_t p_s n + p_2\left(n^2\sqrt{E^2+\Gamma_t^2}+\frac{p_s^2}{m_t}\right)}{\left(E+\frac{p_s^2}{m_t n^2}\right)^2+\Gamma_t^2} ,$$

$$\tilde{G}^{(8)}(E) = \frac{4\pi}{m_t^2}\Im G^{(8)}_{E+i\Gamma_t}(0,0) = \frac{p_2}{m_t} + \frac{2p_8}{m_t}\arctan\frac{p_2}{p_1} + \frac{2p_8^2}{m_t^2}\sum_{n=1}^{\infty}\frac{m_t p_2}{(np_1-p_8)^2+n^2p_2^2} ,$$

$$\text{where} \quad p_s = \frac{2}{3}m_t\alpha_s ,$$

$$p_8 = -\frac{1}{12}m_t\alpha_s ,$$

$$p_{1,2} = \sqrt{\frac{m_t}{2}\left(\sqrt{E^2+\Gamma_t^2}\mp E\right)} .$$

The singlet channel $\tilde{G}^{(s)}(E)$

1990: top not yet found, so results for $m_{\mathrm{t}} = 100$, 140 and **200** GeV.

1990:

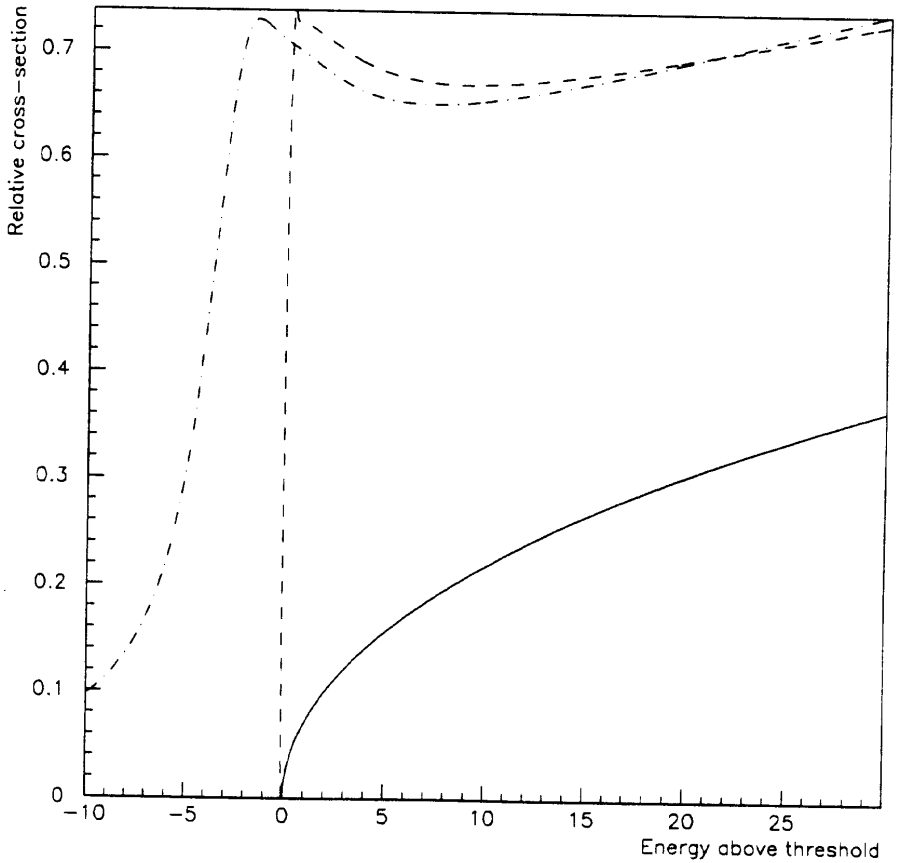

2025:

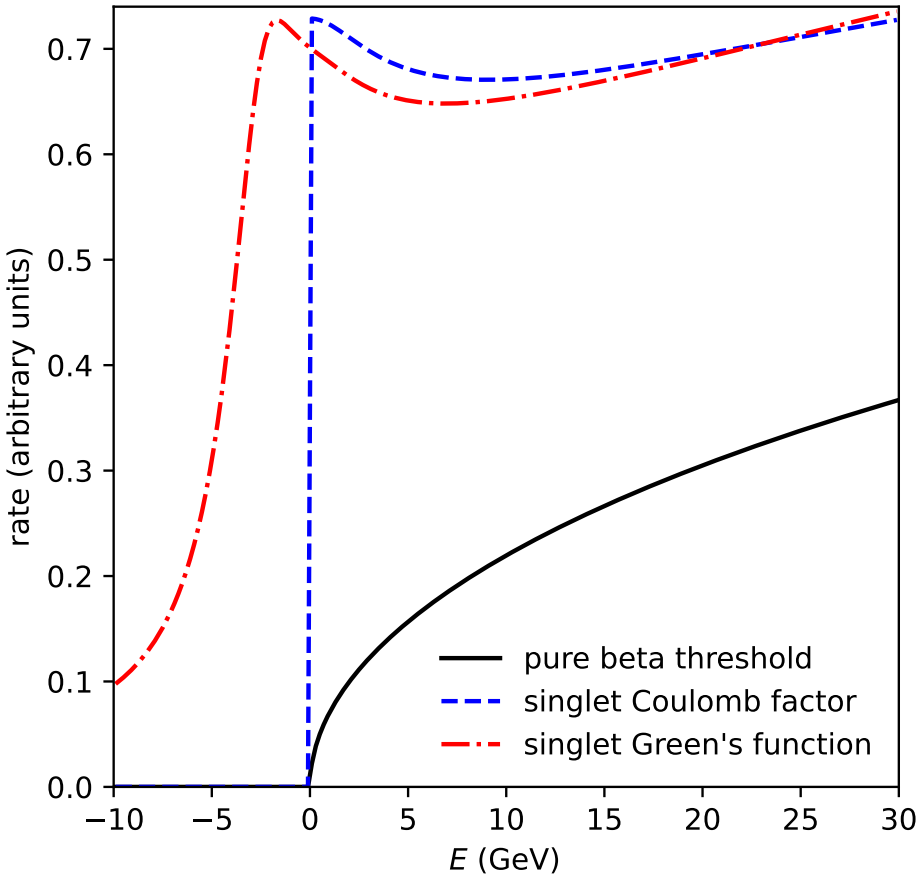

Note values at the time: $\Gamma_{\mathrm{t}} = 2.5$ GeV for $m_{\mathrm{t}} = 200$ GeV;
$\Lambda^{(5)}_{\mathrm{QCD}} = 0.2$ GeV $\Rightarrow \alpha_{\mathrm{s}}(m_{\mathrm{Z}}^2) = 0.134$.

The octet channel $\tilde{G}^{(8)}(E)$

1990: top not yet found, so results for $m_{\mathrm{t}} = 100$, 140 and **200** GeV.

1990:

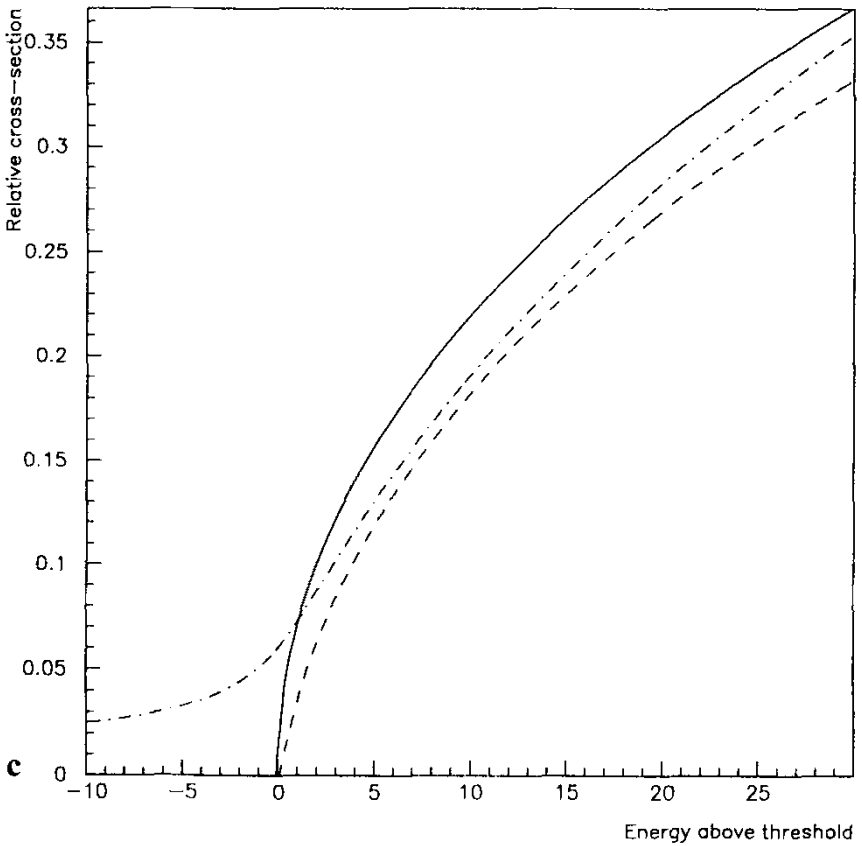

2025:

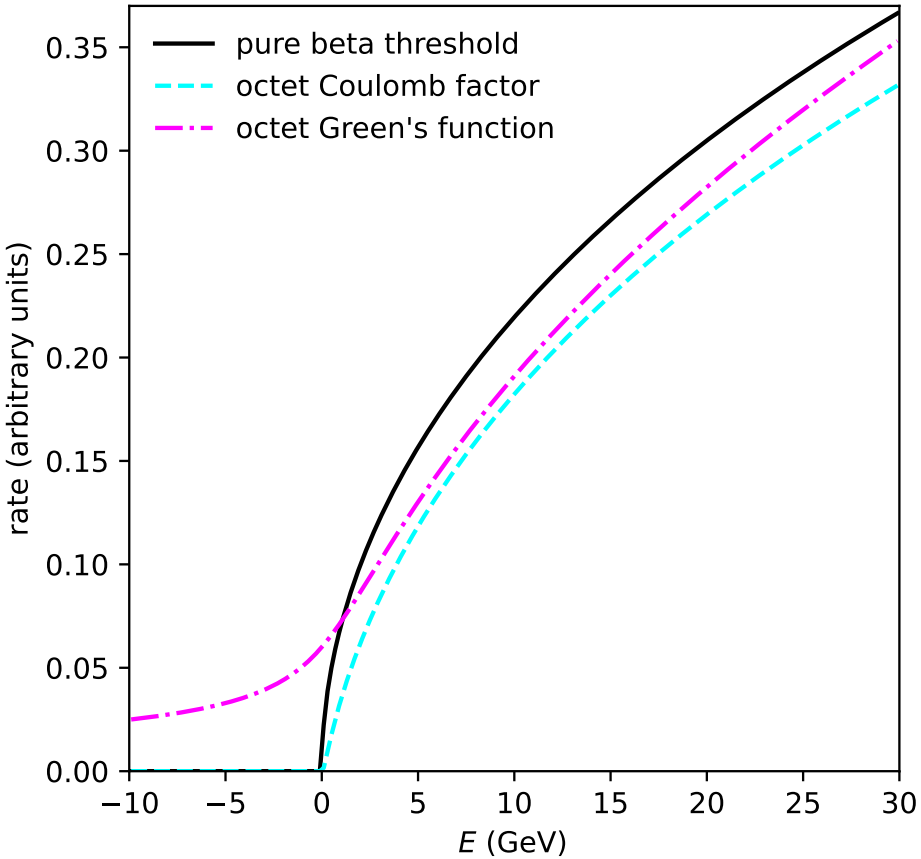

Note values at the time: $\Gamma_{\mathrm{t}} = 2.5$ GeV for $m_{\mathrm{t}} = 200$ GeV;
$\Lambda^{(5)}_{\mathrm{QCD}} = 0.2$ GeV $\Rightarrow \alpha_{\mathrm{s}}(m_{\mathrm{Z}}^2) = 0.134$.

Singlet and octet channels for current top mass

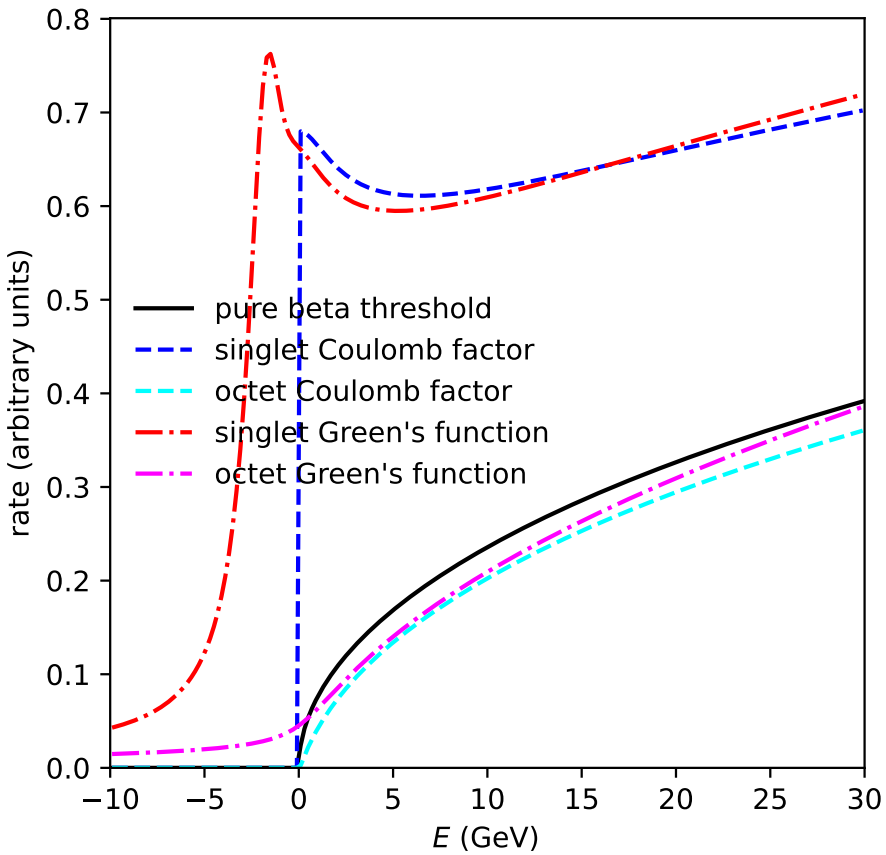

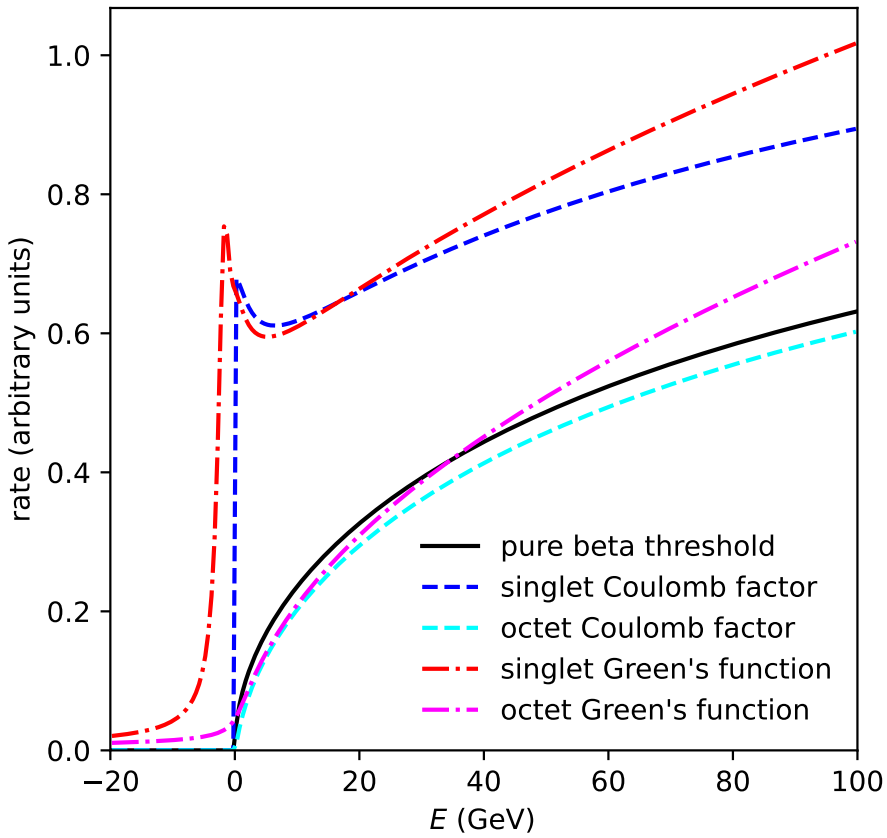

$m_t = 200 \to 172.5$ GeV,
$\Gamma_t = 2.5 \to 1.34$ GeV,
$\alpha_s(m_Z^2) = 0.134 \to 0.118$
with $1 \to 2$ order running.

Green's only reliable near $E = 0$:
e.g. dampen to 0 between
$E = -10$ and -20 GeV.
What about large E?

Corrected threshold

In FK Green's functions, E is nonrelativistic limit of $m_t\beta_t^2$:

$$E = (\hat{m} - 2m_t)\left(\frac{\hat{m} + 2m_t}{\hat{m} + 2m_t}\right)$$
$$= \frac{\hat{s} - 4m_t^2}{\hat{m} + 2m_t} \approx m_t\left(1 - 4\frac{m_t^2}{\hat{s}}\right)$$

so define "Green" E_G accordingly

$$E_G = \hat{m} - m_{t1} - m_{t2}$$
$$\to \overline{m}_t\left((1 - r_1 - r_2)^2 - 4r_1r_2\right)$$

with $r_1 = m_{t1}^2/\hat{s}$ and $r_2 = m_{t2}^2/\hat{s}$.

Intended to work also for $\beta^2 < 0$!

With $\tilde{G}^{(s,8)}(E) \to \tilde{G}^{(s,8)}(E_G(E))$:

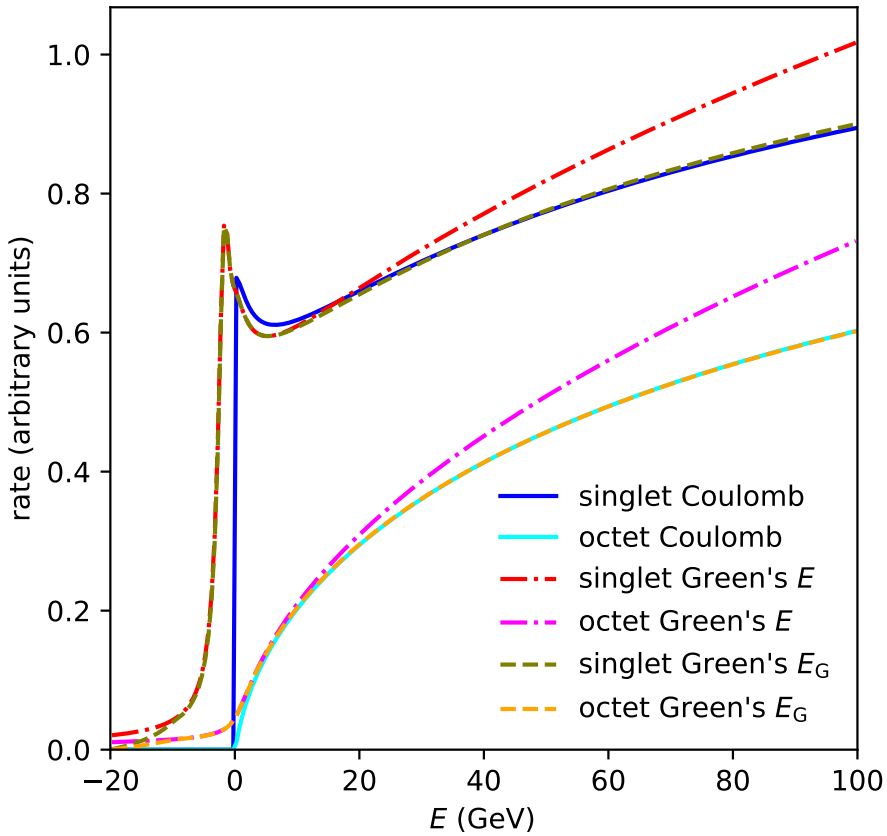

With damping for $E < -10$ GeV.

What does $E < 0$ mean for events?

In the Green's function Γ_{t} is a parameter,
but $\mathrm{t}/\bar{\mathrm{t}}$ Breit-Wigner (BW) mass smearing is not explicit (but . . .).
And the fate of a below-threshold state is not detailed.

In a complete description — like in an event generator —
the above-threshold part is straightforward: pick events according to
$\mathrm{BW}(\mathrm{t}) \times \mathrm{BW}(\bar{\mathrm{t}}) \times \mathrm{PDF}(x_1) \times \mathrm{PDF}(x_2) \times \mathrm{ME} \times \mathrm{PS} \times \tilde{G}(E_{\mathrm{G}})/\beta_{\mathrm{t}}$
(PDF = parton distribution, ME = matrix element, PS = phase space).

Does not work for $E < 0$, where phase space is vanishing naively.
But an $E < 0$ pseudo-bound state decays by the weak decays of t and $\bar{\mathrm{t}}$.
A theorist's detector would reconstruct $m'_{\mathrm{t}1}$ and $m'_{\mathrm{t}2}$
where $m'_{\mathrm{t}1} + m'_{\mathrm{t}2} < m_{\mathrm{t}1} + m_{\mathrm{t}2}$ so that $E' = \hat{m} - m'_{\mathrm{t}1} - m'_{\mathrm{t}2} > 0$.
$\Rightarrow$ the $E < 0$ states are never detectable as such,
but show up as a component of the BW with lower average mass.

So ideally correctly modified BWs would solve it, but no such known (?).
How handle in practice?

The four-mass "hybrid" solution

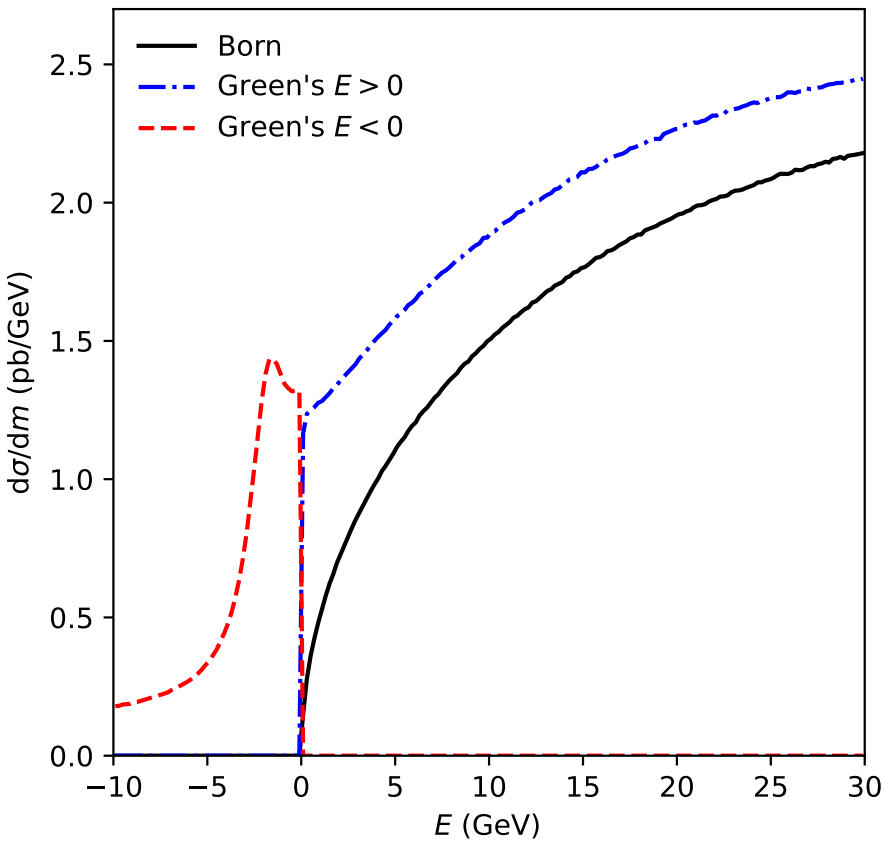

Full simulation pp at 13 TeV,
300 GeV $< \hat{m} <$ 400 GeV.
$\mathrm{gg} \to \mathrm{t\bar{t}}$ 2/7 singlet, 5/7 octet.
$\mathrm{q\bar{q}} \to \mathrm{t\bar{t}}$ all octet.

1. BW-pick $m_{\mathrm{t}1}$, $m_{\mathrm{t}2}$.
2. Pick $\hat{m} > m_{\mathrm{t}1} + m_{\mathrm{t}2} - 20$ GeV.
3. If $E < 0$ BW-pick $m'_{\mathrm{t}1} < m_{\mathrm{t}1}$, $m'_{\mathrm{t}2} < m_{\mathrm{t}2}$ such that $E' > 0$.
4. If $E > 0$ weigh by $\tilde{G}(E_{\mathrm{G}})/\beta_{\mathrm{t}}$, else by "hybrid" $\tilde{G}(E_{\mathrm{G}})/\beta'_{\mathrm{t}}$.

Advantages:
realistic E, $\hat{m}$, $m'_{\mathrm{t}1}$, $m'_{\mathrm{t}2}$ and β'_{t} distributions.

Disadvantages:
ad hoc $m'_{\mathrm{t}1}$ and $m'_{\mathrm{t}2}$ selection, affecting $E < 0$ weighting;
tiny mismatch at $E = 0$.

$\sigma(E < 0) = 6.76$ pb.

Kinematics distributions – 1

Invariant mass of $\mathrm{t} + \bar{\mathrm{t}}$ pair:

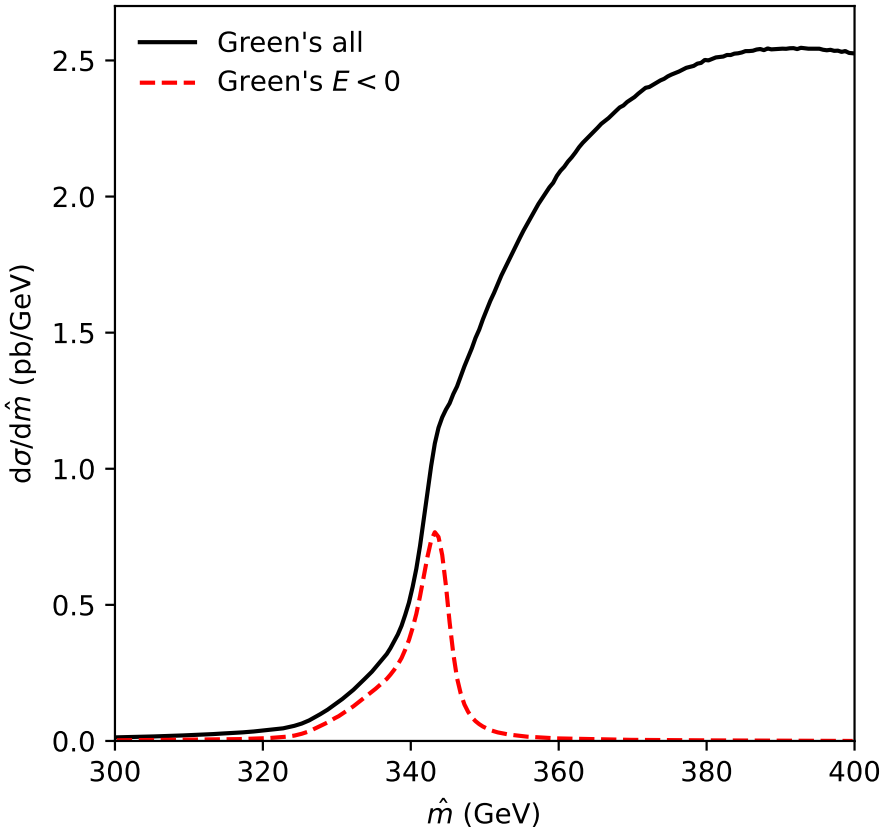

Breit-Wigners smear
meaning of threshold at $2m_{\mathrm{t}}$.

Ditto, but all masses > 200 GeV:

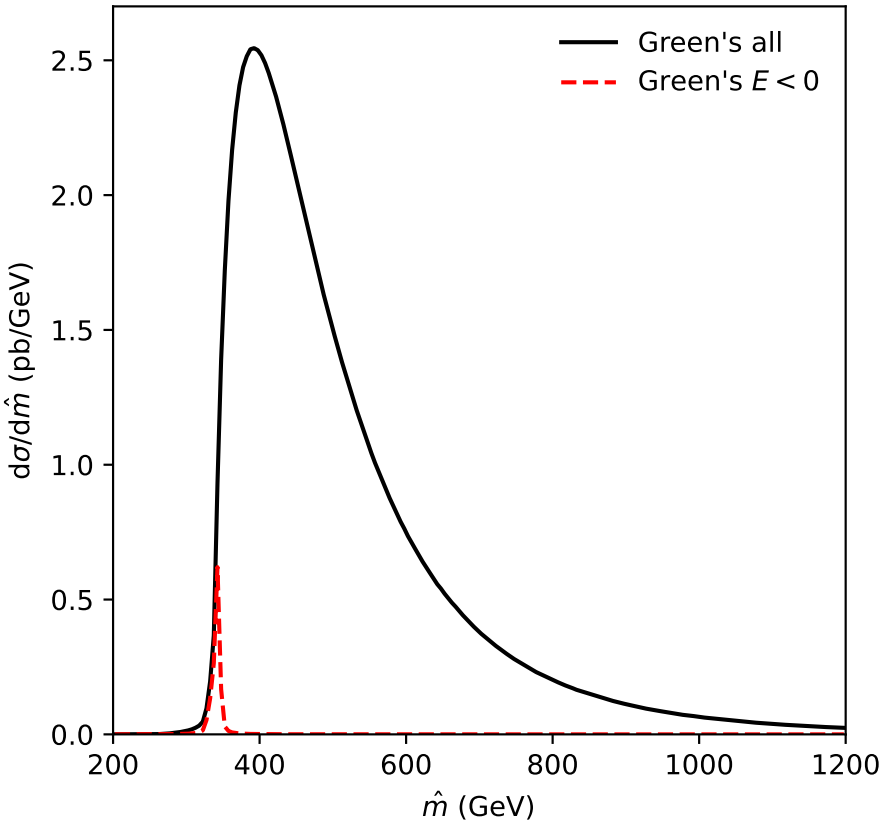

In full range $\sigma_{\mathrm{tot}} = 565$ pb,
so $\sigma_{E<0} = 6.76$ pb $= 1.2\%$.

Kinematics distributions – 2

Actual masses of t and $\bar{\mathrm{t}}$:

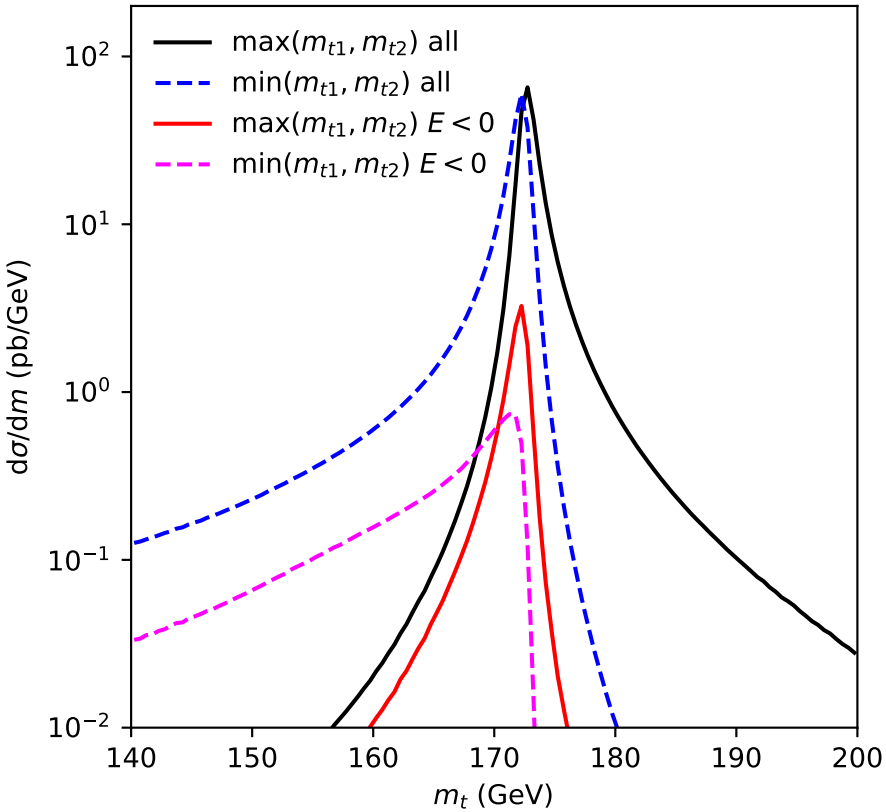

$E < 0$ contribution typically leaves heavier $\mathrm{t}/\bar{\mathrm{t}}$ close to peak, while lighter is pushed off-shell.

Average velocity β_{t} of the pair:

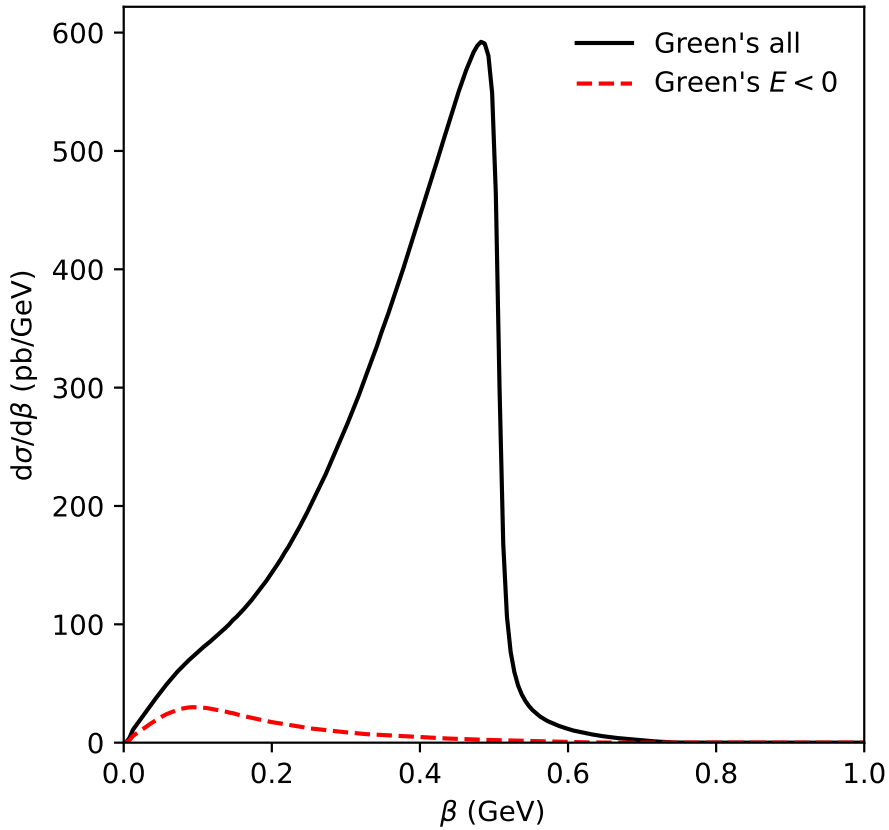

As expected below-threshold top quarks typically are slow-moving. (These plots for $300 < \hat{m} < 400$.)

The Breit–Wigner threshold smearing

PYTHIA operates in a "narrow width approximation":

$$\mathrm{d}\hat{\sigma}(\hat{s}, m_{\mathrm{t}1}, m_{\mathrm{t}2}) = \mathrm{BW}(m_{\mathrm{t}1}) \times \mathrm{BW}(m_{\mathrm{t}2}) \times \mathrm{d}\hat{\sigma}(\hat{s}, \overline{m}).$$

Straightforward when $\mathrm{d}\hat{\sigma}(\hat{s}, \overline{m})$ is independent of Γ_{t}:

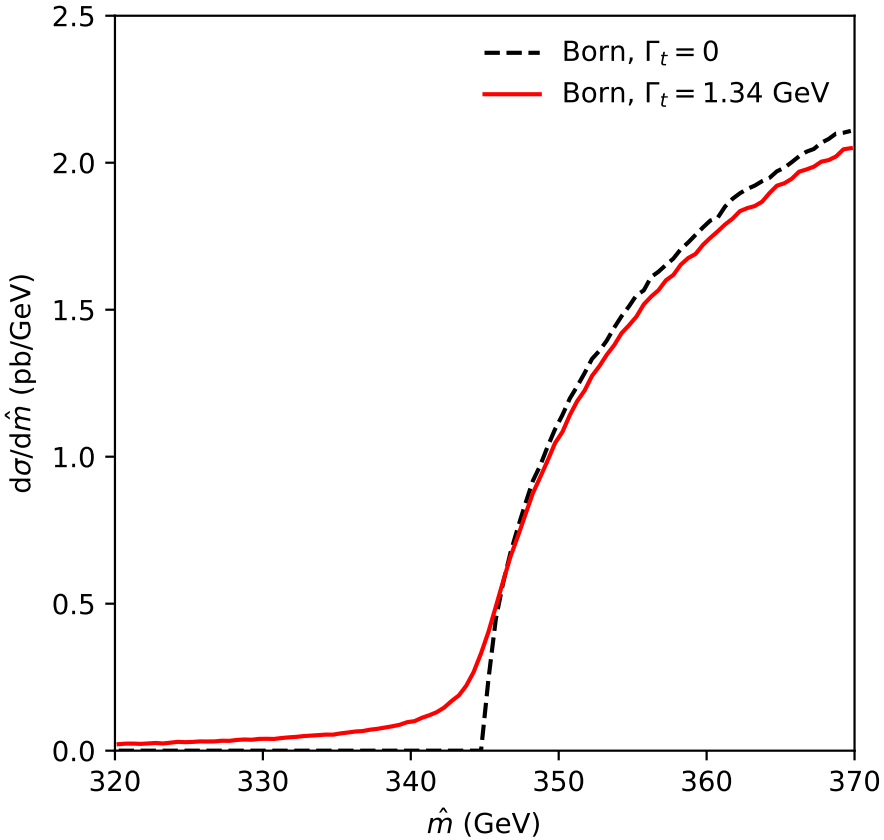

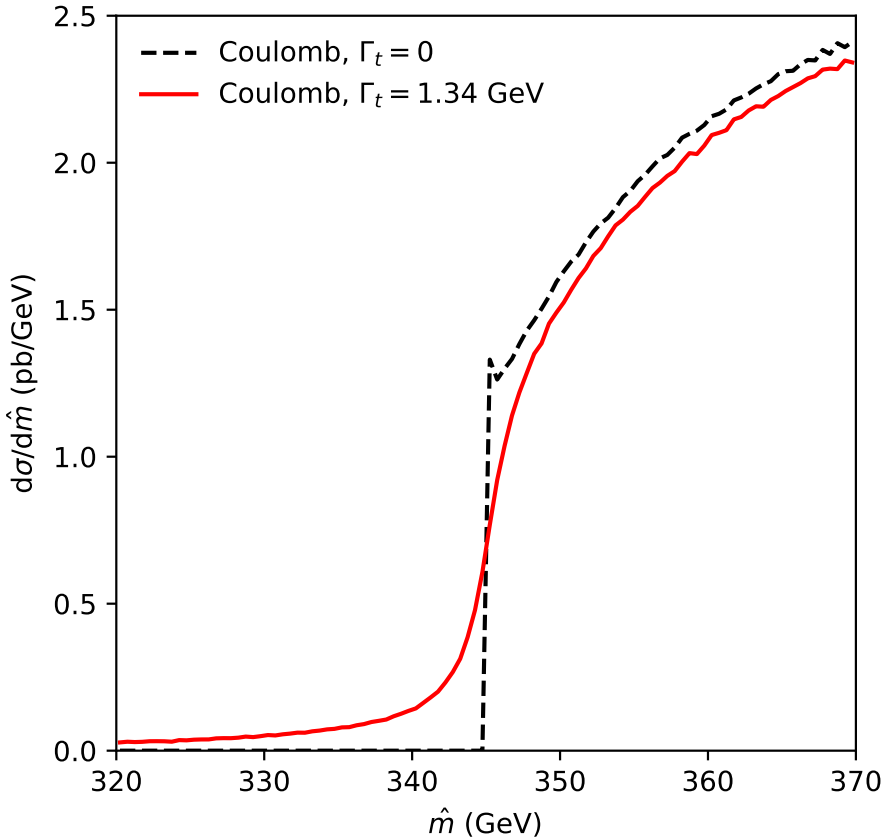

But what to do when Γ_{t} dependence is less trivial?

Width doublecounting issues

So far the "full" Green's handling has involved several scale choices:

1. Event-by-event Breit-Wigner $m_{\mathrm{t}1}$ and $m_{\mathrm{t}2}$ define $E = 0$ level.
2. Almost discrete $E < 0$ pseudo-bound state locations, given by the QCD potential, with a negligible ~ 2 MeV QCD decay width.
3. Full width of the pseudo-bound states, approximately $2\Gamma_{\mathrm{t}}$.
4. Conditional Breit-Wigners $m'_{\mathrm{t}1}$ and $m'_{\mathrm{t}2}$ when $E < 0$.

Is there doublecounting?

Yes, unfortunately!

See e.g. V.S. Fadin and V.A. Khoze, Sov.J.Nucl.Phys. 53 (1991) 692, where Born-level cross section factor β_{t} becomes p_2/m_{t} by BW smearing. (Though not perfect agreement.)

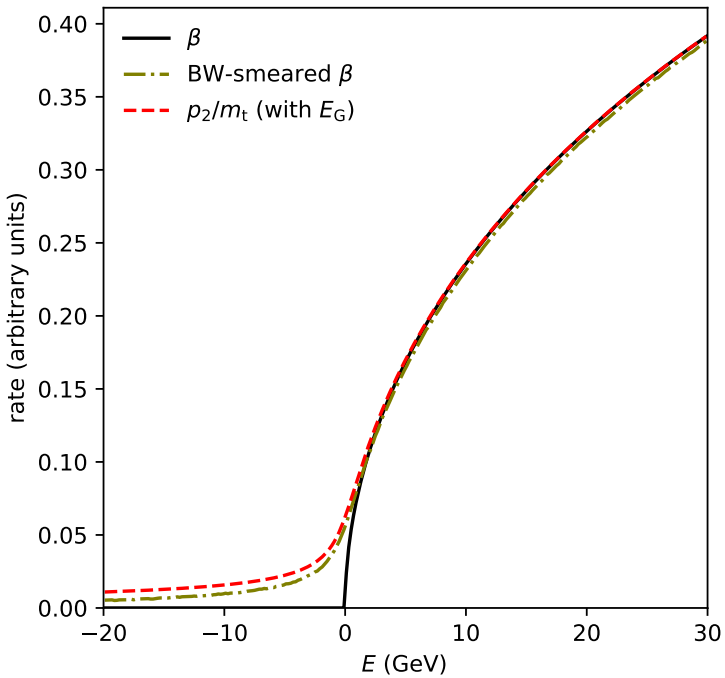

Width doublecounting distributions

How eliminate/reduce doublecounting between explicit BWs and Green's-function-corrected MEs?
Setting $\Gamma_{\mathrm{t}}^{\mathrm{BW}} = 0$ or $\Gamma_{\mathrm{t}}^{\mathrm{ME}} = 0$ gives singularities in the PYTHIA code, so not possible, but e.g $\Gamma_{\mathrm{t}} = 0.2$ GeV works.

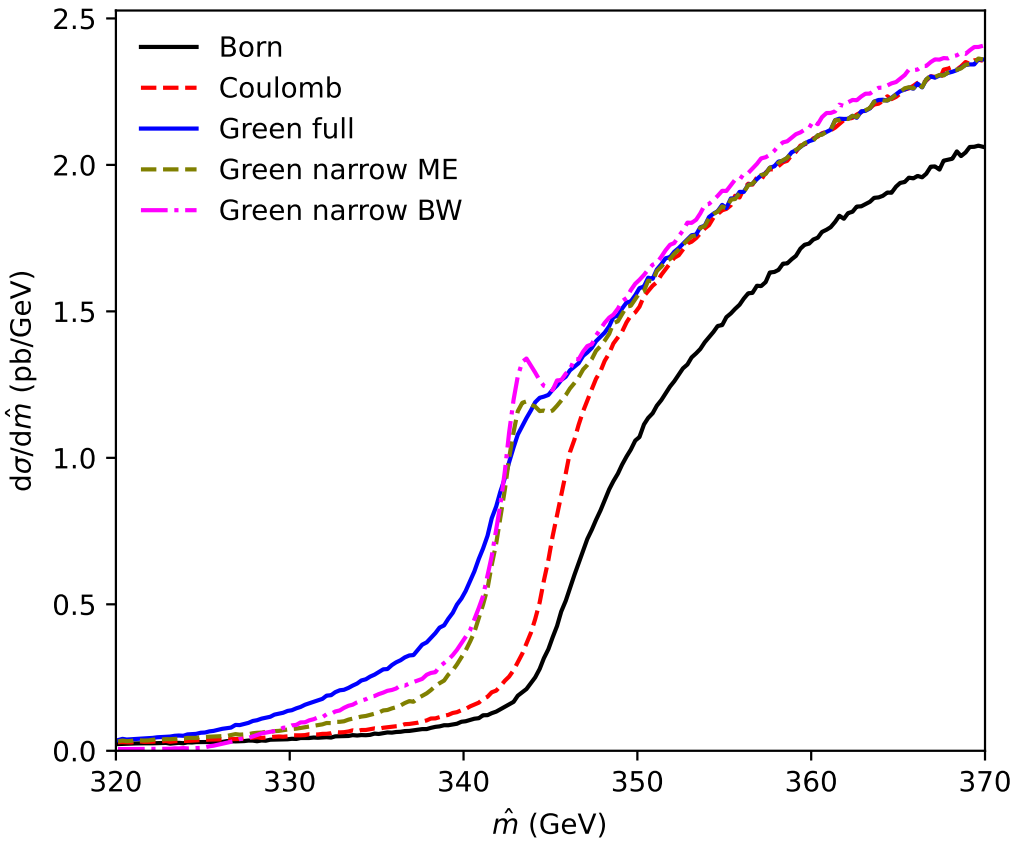

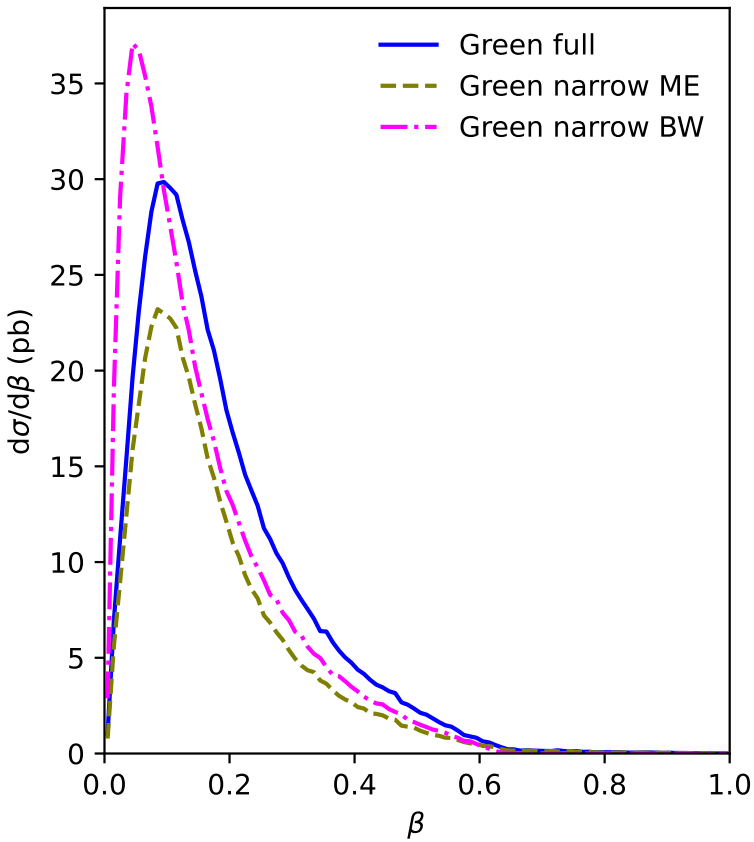

Cross sections

	σ (pb)			
model	$E < 0$	$\hat{m} < 345$	$\hat{m} < 380$	all
Born	0.00	2.23	61.313	516.26
Coulomb	0.00	3.21	74.35	558.58
Green full	6.78	8.85	81.07	565.10
Green narrow ME	4.74	6.85	78.86	562.98
Green narrow BW	6.67	6.98	80.79	569.35
gg only	6.32	8.08	70.42	502.05
$\mathrm{q\overline{q}}$ only	0.46	0.76	10.63	63.06
gg singlet + $\mathrm{q\overline{q}}$ octet	17.92	20.90	140.26	744.65
gg octet + $\mathrm{q\overline{q}}$ octet	2.34	4.05	57.38	493.25
ME $\alpha_{\mathrm{s}}^{(1)} = 0.130$ $\rightarrow \alpha_{\mathrm{s}}^{(2)} = 0.118$	5.64	7.36	67.45	471.38
PDF NNPDF 2.3 LO $\rightarrow$ PDF4LHC21 NNLO	6.93	9.05	83.74	584.10

Angular distributions (1)

For pseudoscalar toponium the t and $\bar{\mathrm{t}}$ are correlated, giving ME

```
double wt = - 16*s13*s25*s46*m2Sq - 16*s13*s25*s46*m1Sq + 16*s13*s25*s45*s56
  + 16*s13*s25*s36*s45 - 16*s13*s25*s35*s46 + 16*s13*s25*s34*s56
  + 16*s13*s25*s34*s36 + 16*s13*s25*s26*s45 + 16*s13*s25*s26*s34
  - 16*s13*pow2(s25)*s46 + 16*s13*s24*s25*s56 + 16*s13*s24*s25*s36
  + 16*s13*s24*s25*s26 - 16*s13*s23*s25*s46 + 16*s13*s16*s25*s45
  + 16*s13*s16*s25*s34 + 16*s13*s16*s24*s25 - 16*s13*s15*s25*s46
  + 16*s13*s14*s25*s56 + 16*s13*s14*s25*s36 + 16*s13*s14*s25*s26
  + 16*s13*s14*s16*s25 - 16*pow2(s13)*s25*s46 - 16*s12*s13*s25*s46
  + eps(p1,p2,p3,p4) * ( 4*s46*s56 + 4*s45*s56 - 4*s36*s56 - 4*s35*s56
    - 4*s26*s45 - 4*s26*s35 + 4*s25*s46 + 4*s25*s36 + 4*s24*s56 - 4*s23*s56
    - 8*s16*s45 - 8*s16*s35 - 2*s16*s25 + 8*s15*s46 + 8*s15*s36 + 2*s15*s26 )
  + eps(p1,p2,p3,p5) * ( 4*s46*m2Sq - 4*s46*m1Sq - 4*s46*s56 - 4*pow2(s46)
    - 4*s45*s46 - 4*s36*s45 + 4*s35*s46 + 4*s34*s56 - 4*s34*s36 + 4*s23*s46
    - 2*s16*s46 - 2*s15*s46 + 2*s14*s56 - 4*s14*s46 - 4*s13*s46 )
  + eps(p1,p2,p3,p6) * ( - 4*s45*m2Sq + 4*s45*m1Sq + 4*s45*s56 + 4*s35*s46
    + 4*s35*s45 + 4*s34*s35 - 4*s24*s45 + 2*s16*s45 + 2*s15*s45 + 2*s14*s56
    + 4*s14*s45 + 4*s13*s45 )
  + eps(p1,p2,p4,p5) * ( -4*s36*m2Sq + 4*s36*m1Sq + 4*s36*s56 + 4*s36*s46
    + 4*s35*s46 + 4*s34*s46 - 4*s23*s36 + 2*s16*s36 + 2*s15*s36 + 4*s14*s36
    + 2*s13*s56 + 4*s13*s36 )
  + eps(p1,p2,p4,p6) * ( - 4*s36*s45 + 4*s35*m2Sq - 4*s35*m1Sq - 4*s35*s56
    + 4*s35*s46 - 4*s35*s36 - 4*pow2(s35) + 4*s34*s56 - 4*s34*s45 + 4*s24*s35
    - 2*s16*s35 - 2*s15*s35 - 4*s14*s35 + 2*s13*s56 - 4*s13*s35 )
  + eps(p1,p2,p5,p6) * (  - 8*s34*s46 - 4*s34*s45 + 4*s34*s36 + 8*s34*s35
    + 4*s24*s34 - 4*s23*s34 - 2*s14*s36 + 2*s14*s35 + 8*s14*s34 + 2*s14*s23
    - 2*s13*s46 + 2*s13*s45 - 8*s13*s34 - 2*s13*s24 )
  + eps(p1,p3,p4,p5) * ( - 8*s26*m1Sq - 8*s26*s56 + 2*s26*s46 - 2*s26*s45
    + 6*s26*s36 + 2*s26*s35 - 8*s26*s34 - 4*pow2(s26) + 4*s25*s46 + 4*s25*s36
    - 4*s25*s26 - 4*s24*s56 - 4*s23*s56 + 4*s23*s26 + 4*s16*m2Sq - 4*s16*s25
    + 4*s15*s26 - 8*s14*s26 - 8*s13*s26 )
  + eps(p1,p3,p4,p6) * ( - 4*s26*s45 - 4*s26*s35 + 8*s25*m1Sq + 8*s25*s56
    - 2*s25*s46 - 6*s25*s45 + 2*s25*s36 - 2*s25*s35 + 8*s25*s34 + 4*s25*s26
    + 4*pow2(s25) + 4*s24*s56 - 4*s24*s25 + 4*s23*s56 - 4*s16*s25 - 4*s15*m2Sq
    + 4*s15*s26 + 8*s14*s25 + 8*s13*s25 )
  + eps(p1,p3,p5,p6) * ( 8*s34*m2Sq + 4*s26*s34 - 4*s24*m2Sq - 4*s24*m1Sq
    - 4*s24*s56 - 2*s24*s46 - 2*s24*s45 - 2*s24*s36 - 2*s24*s35 - 8*s24*s34
    - 4*s24*s26 - 4*s24*s25 - 4*pow2(s24) + 4*s23*s34 - 4*s23*s24 + 6*s16*s24
    + 6*s15*s24 - 2*s14*s26 - 6*s14*s25 - 12*s14*s24 - 8*s14*s23 - 4*s13*s24
    + 8*s12*s34 + 2*s12*s24 )
  + eps(p1,p4,p5,p6) * ( - 8*s34*m2Sq - 4*s25*s34 - 4*s24*s34 + 4*s23*m2Sq
    + 4*s23*m1Sq + 4*s23*s56 + 2*s23*s46 + 2*s23*s45 + 2*s23*s36 + 2*s23*s35
    + 8*s23*s34 + 4*s23*s26 + 4*s23*s25 + 4*s23*s24 + 4*pow2(s23) - 6*s16*s23
    - 6*s15*s23 + 4*s14*s23 + 6*s13*s26 + 2*s13*s25 + 8*s13*s24 + 12*s13*s23
    - 8*s12*s34 - 2*s12*s23 )
  + eps(p2,p3,p4,p5) * ( - 8*s56*m1Sq + 16*s46*m1Sq + 16*s36*m1Sq
    + 24*s16*m2Sq + 8*s16*m1Sq + 8*s16*s56 - 2*s16*s46 - 2*s16*s45
    - 6*s16*s36 - 6*s16*s35 + 8*s16*s34 + 20*s16*s26 + 4*s16*s25 + 4*s16*s24
    - 4*pow2(s16) + 16*s15*s26 - 4*s15*s16 + 4*s14*s46 - 4*s14*s26
    + 4*s13*s36 - 4*s13*s26 + 4*s12*s26 - 2*s12*s16 )
  + eps(p2,p3,p4,p6) * ( 8*s56*m1Sq - 16*s45*m1Sq - 16*s35*m1Sq - 16*s16*s25
    - 24*s15*m2Sq - 8*s15*m1Sq - 8*s15*s56 + 6*s15*s46 + 6*s15*s45
    + 2*s15*s36 + 2*s15*s35 - 8*s15*s34 - 4*s15*s26 - 20*s15*s25 - 4*s15*s23
    + 4*s15*s16 + 4*pow2(s15) - 4*s14*s45 + 4*s14*s25 - 4*s13*s35 + 4*s13*s25
    - 4*s12*s25 + 2*s12*s15 )
  + eps(p2,p3,p5,p6) * ( - 8*s46*m1Sq - 8*s45*m1Sq - 4*s24*m1Sq + 16*s16*s24
    + 4*s15*s34 + 16*s15*s24 + 28*s14*m2Sq + 4*s14*m1Sq + 4*s14*s56
    - 6*s14*s46 - 6*s14*s45 - 2*s14*s36 - 2*s14*s35 + 8*s14*s34 + 4*s14*s26
    + 4*s14*s25 + 4*s14*s24 + 4*s14*s23 - 8*s14*s16 - 4*s14*s15 + 4*pow2(s14)
    - 4*s13*s46 - 4*s13*s45 + 4*s13*s14 - 4*s12*s34 + 4*s12*s24 )
  + eps(p2,p4,p5,p6) * ( 8*s36*m1Sq + 8*s35*m1Sq + 4*s23*m1Sq - 4*s16*s34
    - 16*s16*s23 - 16*s15*s23 + 4*s14*s36 + 4*s14*s35 - 28*s13*m2Sq
    - 4*s13*m1Sq - 4*s13*s56 + 2*s13*s46 + 2*s13*s45 + 6*s13*s36 + 6*s13*s35
    - 8*s13*s34 - 4*s13*s26 - 4*s13*s25 - 4*s13*s24 - 4*s13*s23 + 4*s13*s16
    + 8*s13*s15 - 4*s13*s14 - 4*pow2(s13) + 4*s12*s34 - 4*s12*s23 )
  + eps(p3,p4,p5,p6) * ( - 16*s26*m1Sq - 16*s25*m1Sq + 32*s16*m2Sq
    - 4*s16*s24 - 4*s16*s23 + 32*s15*m2Sq - 4*s15*s24 - 4*s15*s23 + 4*s14*s26
    + 4*s14*s25 + 4*s14*s24 + 4*s13*s26 + 4*s13*s25 + 4*s13*s23 + 32*s12*m2Sq
    - 4*s12*s46 - 4*s12*s45 - 4*s12*s36 - 4*s12*s35 );
```

(neglecting separately simulated Breit-Wigners).

Thanks to Christian Preuss

Not calculated: transition away from pure pseudoscalar behaviour.
Instead user-settable begin and end of transition region.

Angular distributions (2)

Pseudoscalar toponium gives strong correlations between ℓ^+ and ℓ^-: $\mathrm{d}P/\mathrm{d}\cos\theta_{\ell^+\ell^-} = (1+\cos\theta_{\ell^+\ell^-})/2$ if $\mathrm{t\bar{t}}$, t and $\bar{\mathrm{t}}$ at rest.

In region with $E < 10$ GeV (incl. $E < 0$) results slightly deformed:

$\cos\theta_{\ell^+\ell^-}$

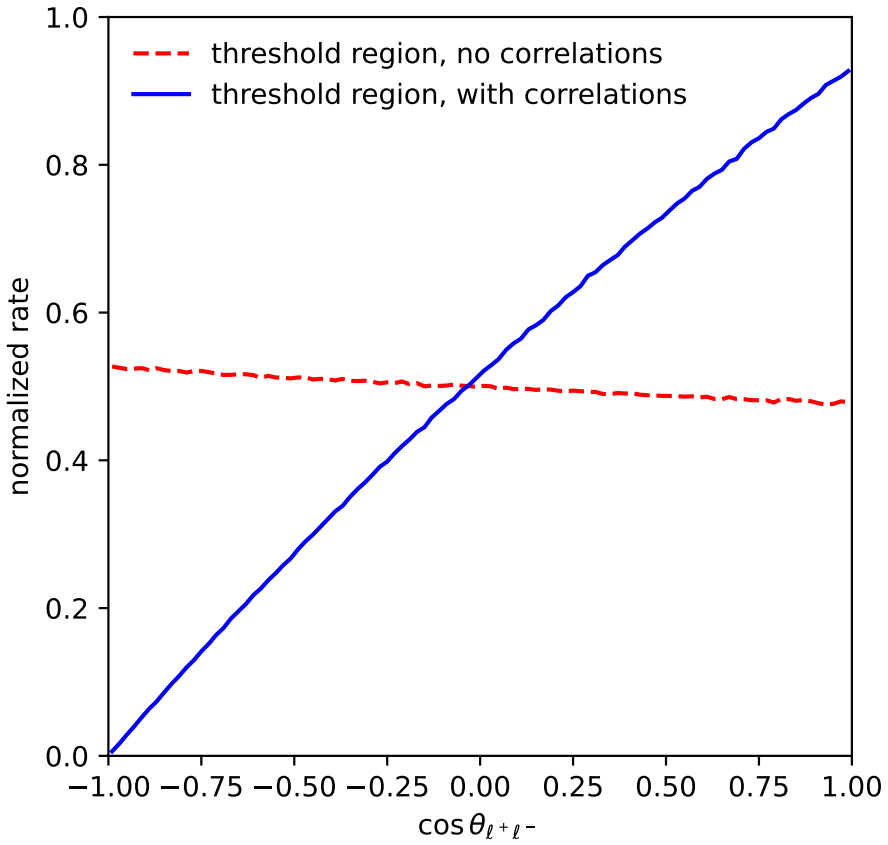

$\cos\theta_{\mathrm{b\bar{b}}}$

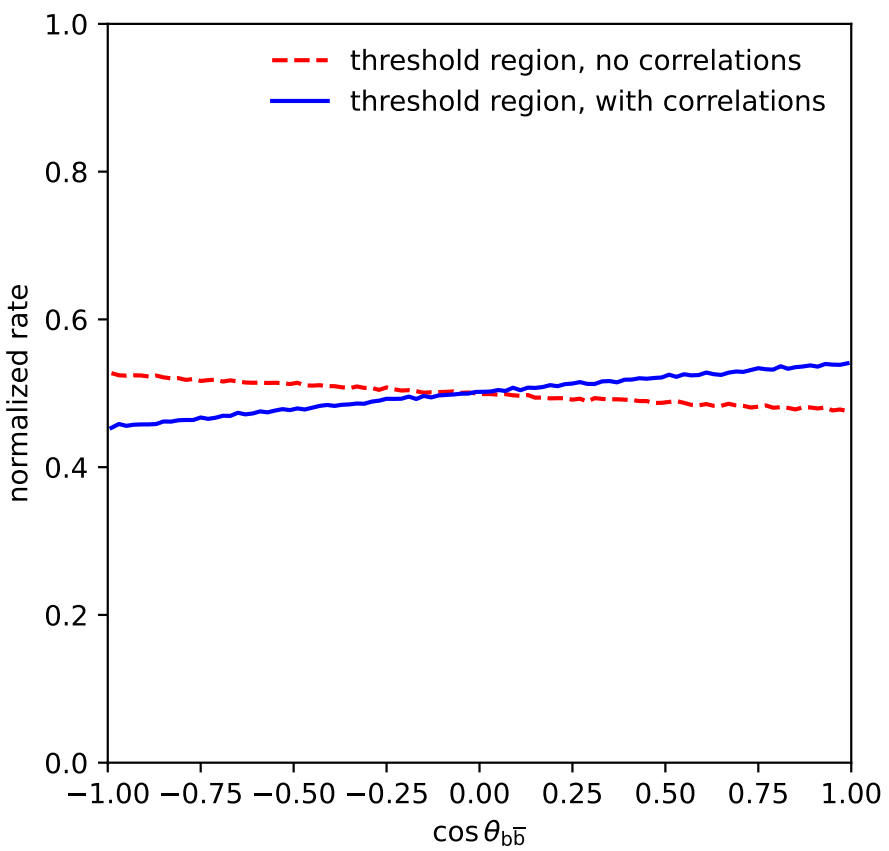

Angular distributions (3)

PYTHIA by default assumes top to be unpolarized,
but in $\mathrm{t} \to \mathrm{bW}^+ \to \mathrm{bf}\bar{\mathrm{f}}'$ decay chain ME $\propto (p_{\mathrm{t}} p_{\bar{\mathrm{f}}'})(p_{\mathrm{f}} p_{\mathrm{b}})$.
Preserved in 6-fermion ME:

$\cos\theta_{\mathrm{b}\ell}$ (same top)

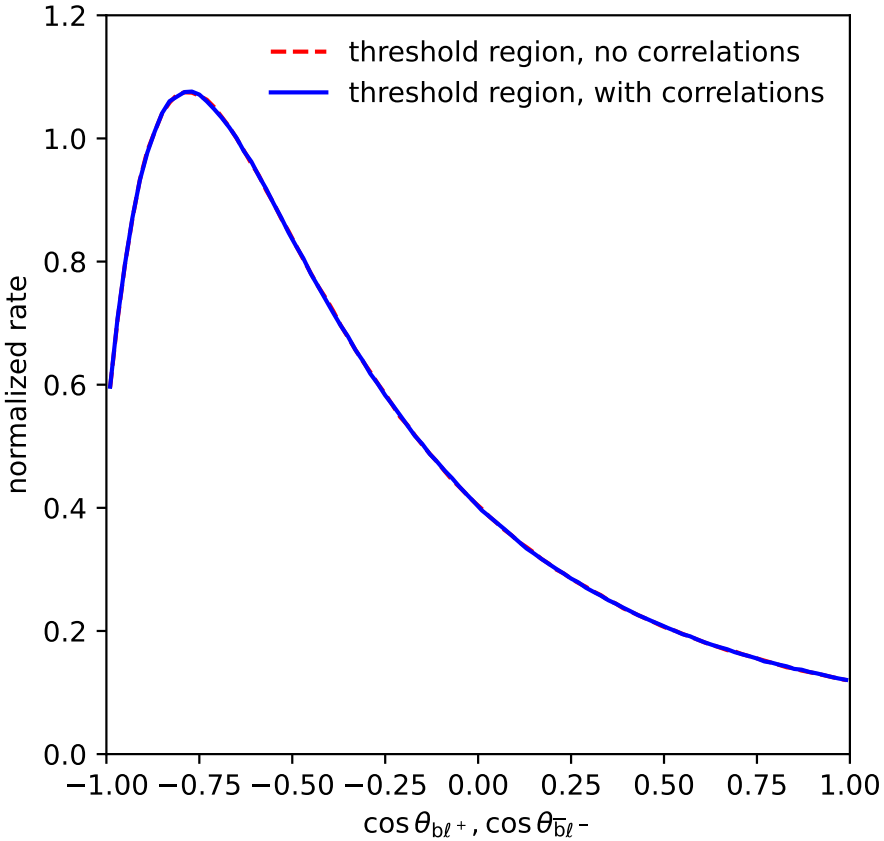

$\cos\theta_{\mathrm{b}\ell}$ (other top)

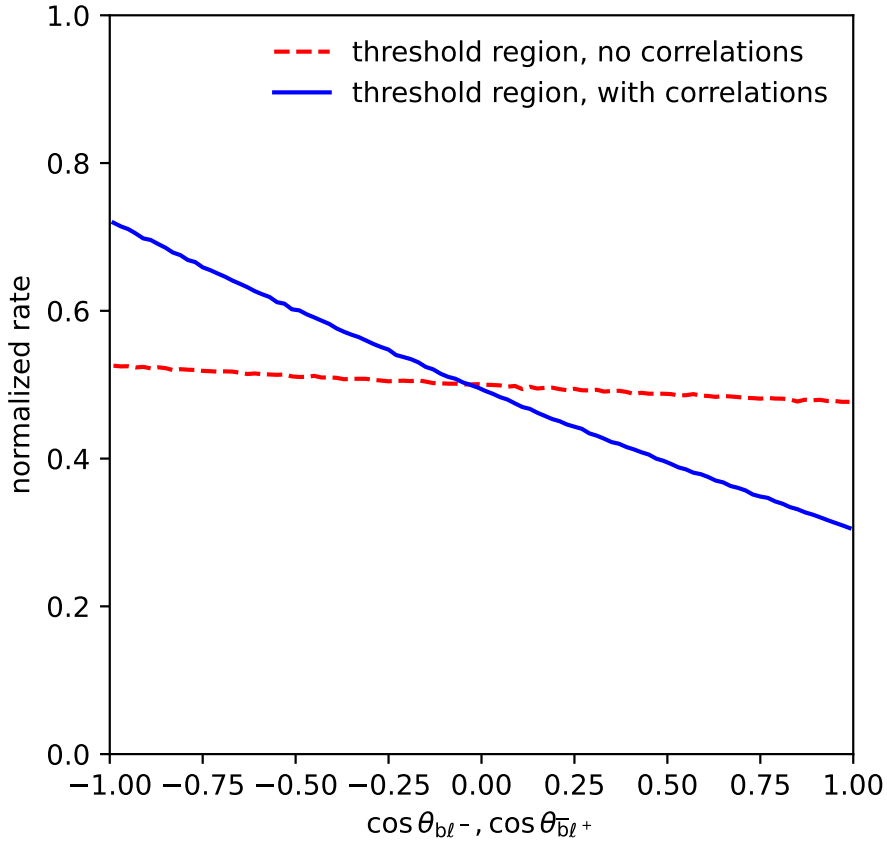

Code status

- PYTHIA 6 contained Coulomb as an option,
  but not Green's since $E < 0$ event generation was not addressed.
- First new code in August as plugin, but simplified below threshold.
- PYTHIA 8.316 in October has full handling of production,
  but still uncorrelated decays.
- Pseudoscalar angular correlations as user hook in November.
  Now integrated into PYTHIA 8.317, released ?? January.
- A few new free parameters: singlet fractions in $\mathrm{gg} \to \mathrm{t\bar{t}}$ and $\mathrm{q\bar{q}} \to \mathrm{t\bar{t}}$,
  threshold region size, α_s in $\tilde{G}(E)$, pseudoscalar decay angles
  + old ones: m_t, Γ_t, PDFs, α_s elsewhere, ...
- All are part of the full PYTHIA event generation chain.
- Nontrivial transition to full (N)NLO somewhat above threshold,
  including consistent top masses and angular decay correlations.

Summary

- Revival of V. Fadin, V. Khoze, TS 1989/1990 study on the top threshold region in pp, based on NRQCD Green's function formalism.
- New extension to generate events in $E < 0$ region, and handle angular distribution of pseudoscalar $\mathrm{t\bar{t}}$ state, now part of PYTHIA 8.317.
- Confusing state of Γ_t handling relevant but not critical.
- **Many** other later calculations, different but in a similar spirit. Could potentially use same framework for other Green's functions.
- Advantage of close integration in a full event generation chain.
- Thanks to **Valery Khoze** and **Christian Preuss**, and

Summary

- Revival of V. Fadin, V. Khoze, TS 1989/1990 study on the top threshold region in pp, based on NRQCD Green's function formalism.
- New extension to generate events in $E < 0$ region, and handle angular distribution of pseudoscalar $\mathrm{t\bar{t}}$ state, now part of PYTHIA 8.317.
- Confusing state of Γ_t handling relevant but not critical.
- **Many** other later calculations, different but in a similar spirit. Could potentially use same framework for other Green's functions.
- Advantage of close integration in a full event generation chain.
- Thanks to **Valery Khoze** and **Christian Preuss**, and

Thank you!

Backup: Examples of 1990 studies

Total cross section, $m_{\mathrm{t}} = 100$ GeV:

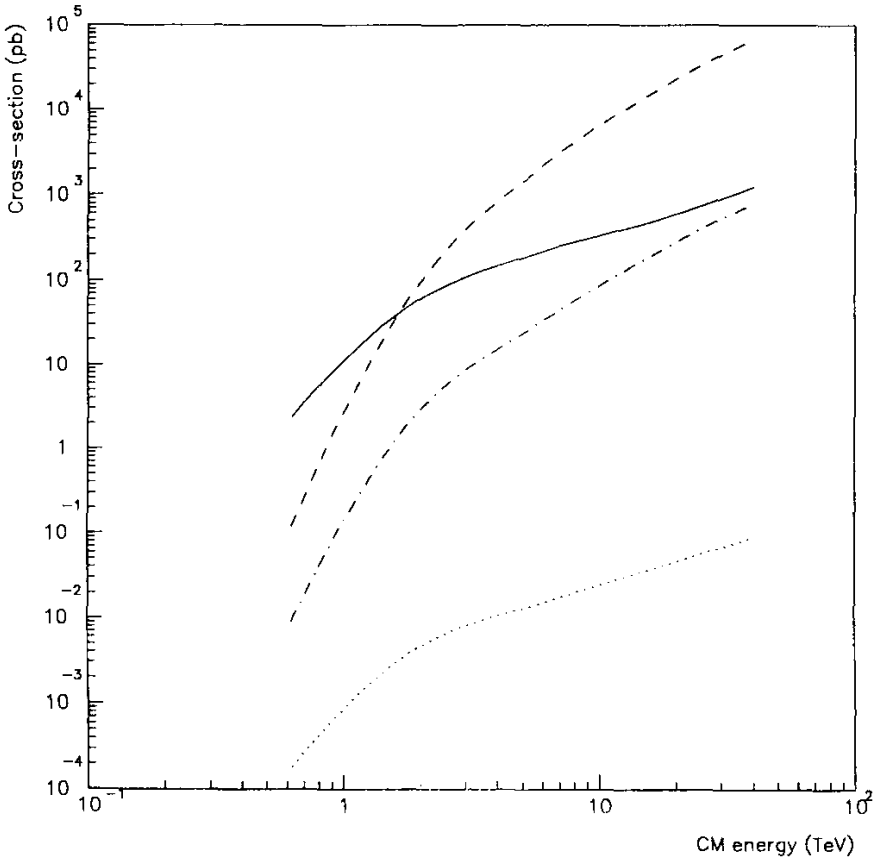

full: $\mathrm{q\bar{q}} \to \mathrm{t\bar{t}}$; dashed: $\mathrm{gg} \to \mathrm{t\bar{t}}$;
dash-dotted: $\mathrm{gg} \to T$:
dotted: $\mathrm{q\bar{q}} \to \mathrm{g}T$ (T = bound)

Differential cross section
for LHC @ 15 TeV, $m_{\mathrm{t}} = 100$ GeV:

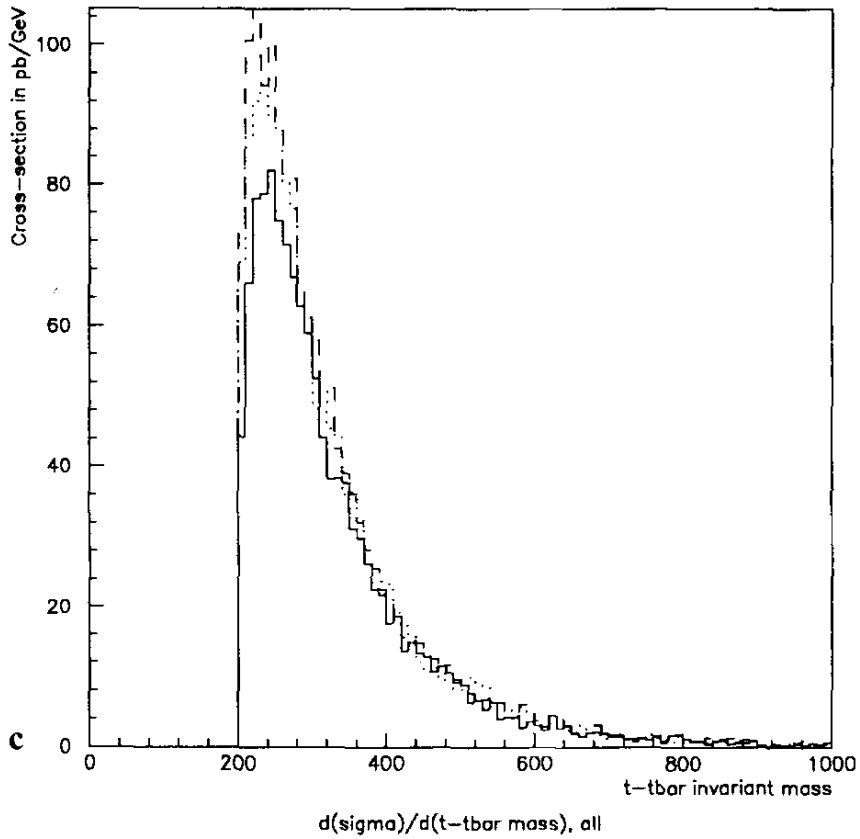

full: Born;
dashed: Coulomb with fixed α_{s};
dotted: Coulomb with running α_{s}

Backup: Green's function breakdown

Recall basic structure with three terms

$$\tilde{G}^{(s,8)}(E) = \frac{p_2}{m_t} + \frac{2p_s}{m_t}\arctan\frac{p_2}{p_1} + \frac{2p_{s,8}^2}{m_t^2}\sum_{n=1}^{\infty}\cdots = \text{term 1} + \text{term 2} + \text{term 3}$$

Colour singlet $\tilde{G}^{(s)}(E_G(E))$

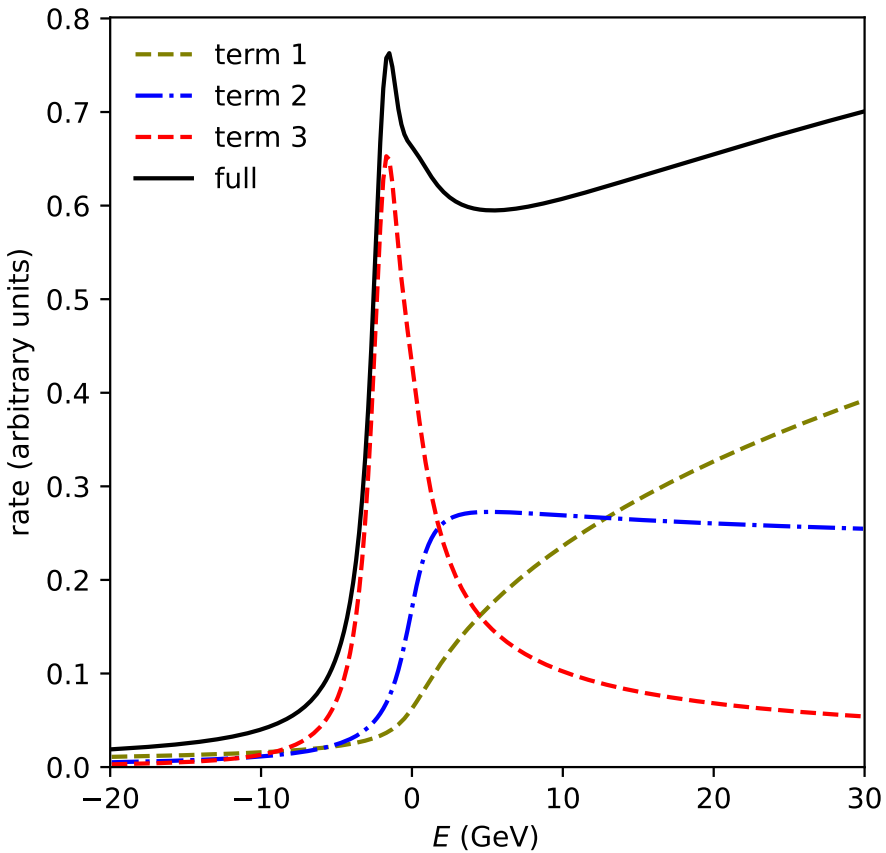

Colour octet $\tilde{G}^{(8)}(E_G(E))$

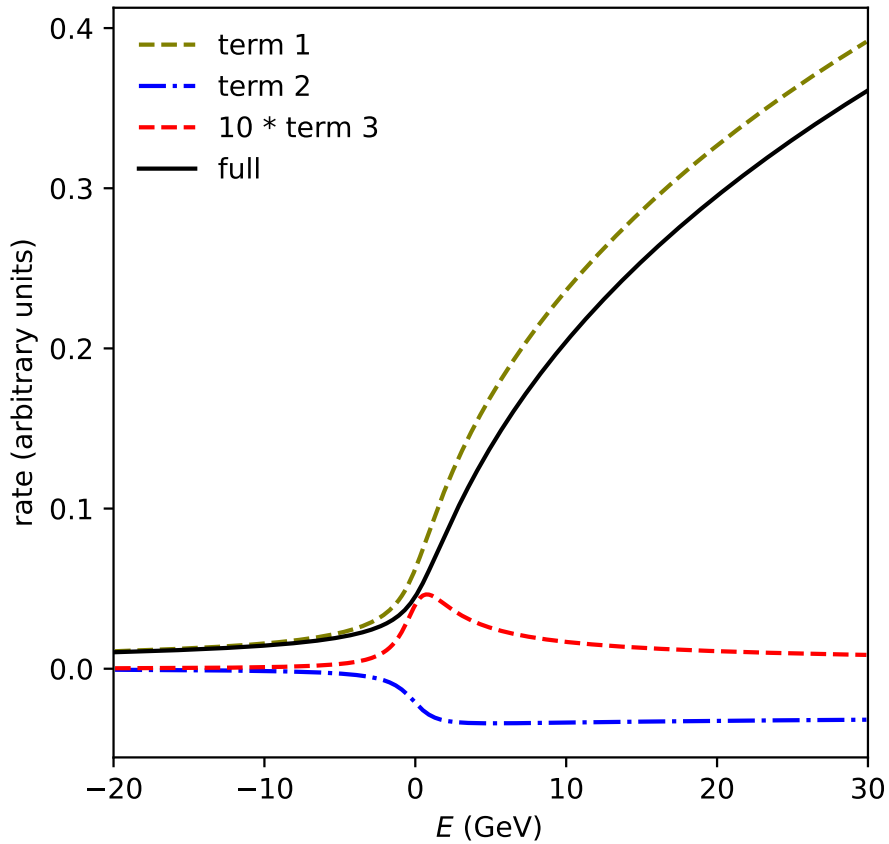

Backup: the threshold region in detail

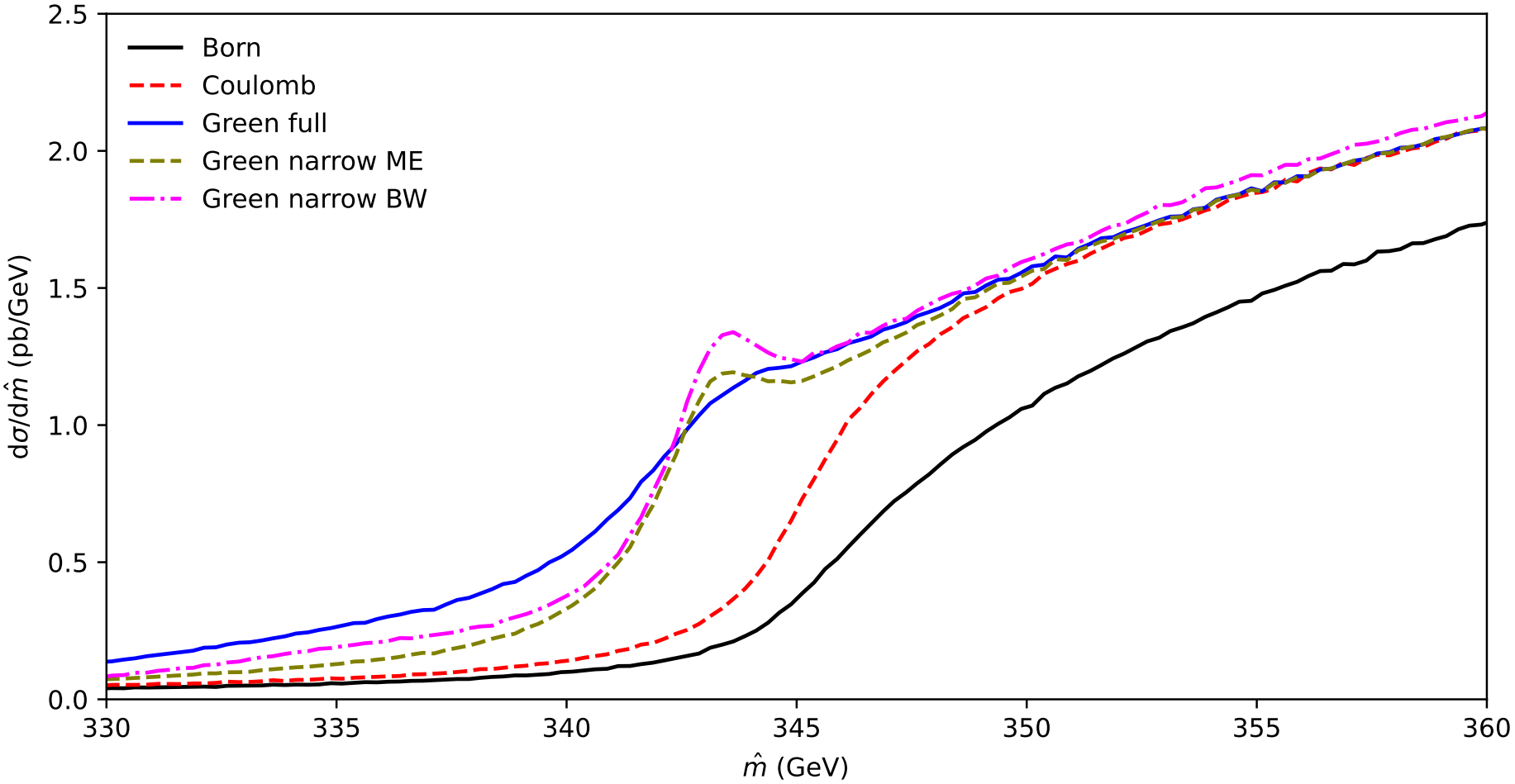

Backup: the UA1 top "signal"

ASSOCIATED PRODUCTION OF AN ISOLATED, LARGE-TRANSVERSE-MOMENTUM LEPTON (ELECTRON OR MUON), AND TWO JETS AT THE CERN $p\bar{p}$ COLLIDER

UA1 Collaboration, CERN, Geneva, Switzerland

A clear signal is observed for the production of an isolated large-transverse-momentum lepton in association with two or three centrally produced jets. The two-jet events cluster around the $W^{\pm}$ mass, indicating a novel decay of the Intermediate Vector Boson. The rate and features of these events are not consistent with expectations of known quark decays (charm, bottom). They are, however, in agreement with the process $W \to t\bar{b}$ followed by $t \to b\ell\nu$, where t is the sixth quark (top) of the weak Cabibbo current. If this is indeed so, the bounds on the mass of the top quark are $30\ \mathrm{GeV}/c^2 < m_t < 50\ \mathrm{GeV}/c^2$.

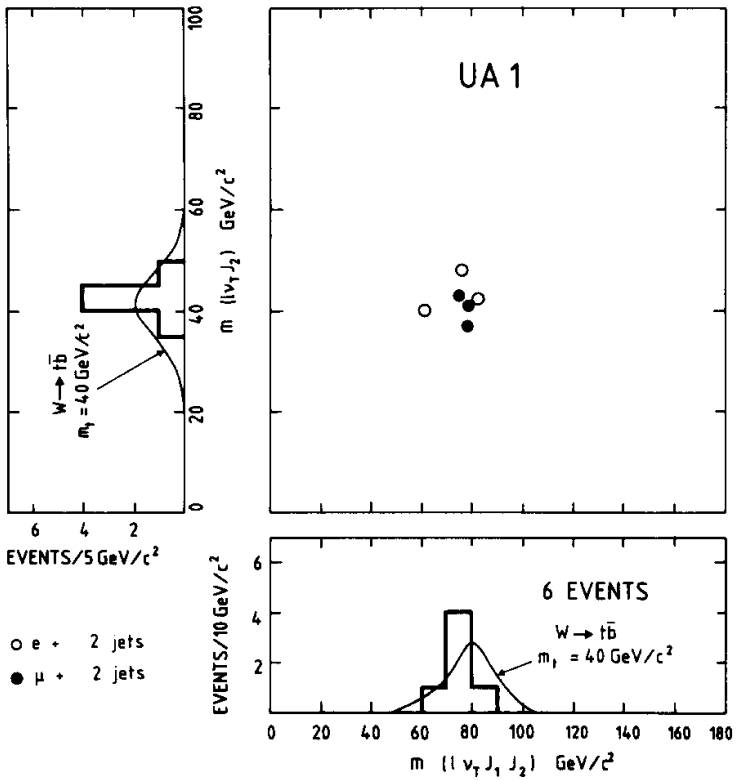

Fig. 10. Four-body versus three-body mass distribution for the six $W \to t\bar{b}$ candidate events. The effective mass of the lepton, the lower-E_T jet, and of the transverse component of the neutrino is plotted against the mass of the lepton, two-jet, transverse neutrino system. The four-body mass peaks at the W mass. The three-body mass clusters around a common value of $\sim 40\ \mathrm{GeV}/c^2$. The curves show the expected [14] distributions, taking into account the experimental resolution. Allowance should be made for a systematic error arising from uncertainties in the jet reconstruction ($\pm 10\ \mathrm{GeV}/c^2$).

Phys.Lett. 147B (1984) 493

Backup: The old mirror alternative

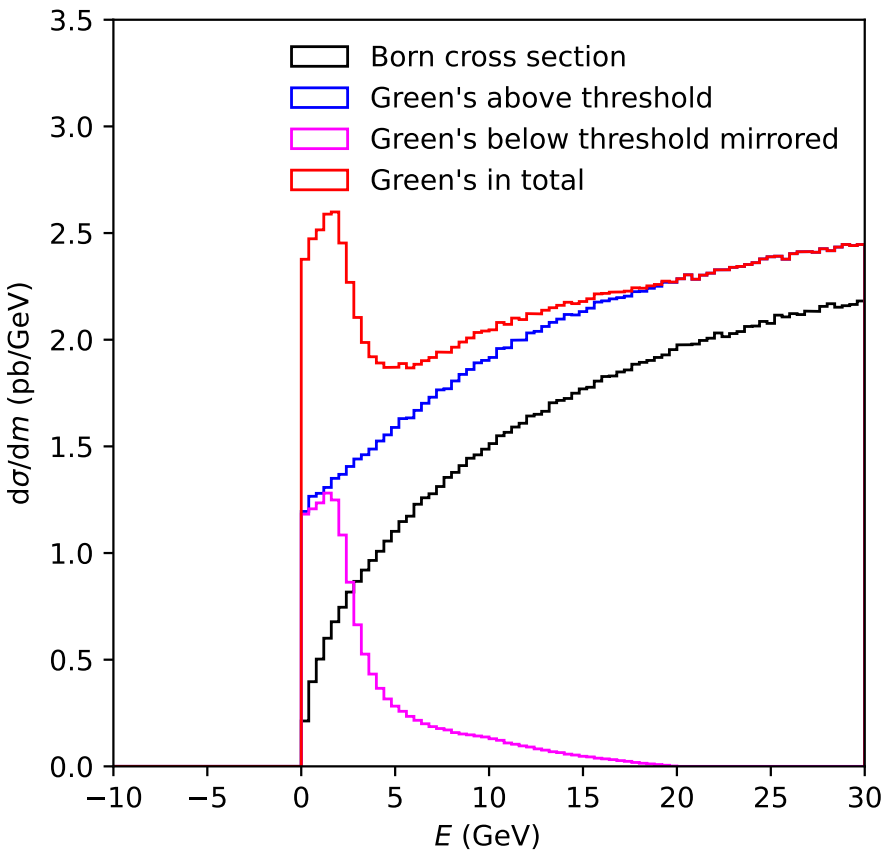

Mirror the $E < 0$ contribution into the $E > 0$ region.

Advantages:
robust Monte-Carlo-wise;
good enough if $\Delta\hat{m} > \mathcal{O}(20\ \mathrm{GeV})$.

Disadvantages:
too low PDF weight
(notably g dropping with x);
no BW distortion.

Full simulation pp at 13 TeV,
300 GeV $< \hat{m} <$ 400 GeV.
$\mathrm{gg} \to \mathrm{t\bar{t}}$ 2/7 singlet, 5/7 octet.
$\mathrm{q\bar{q}} \to \mathrm{t\bar{t}}$ all octet.

Backup: The old mass shift anternative

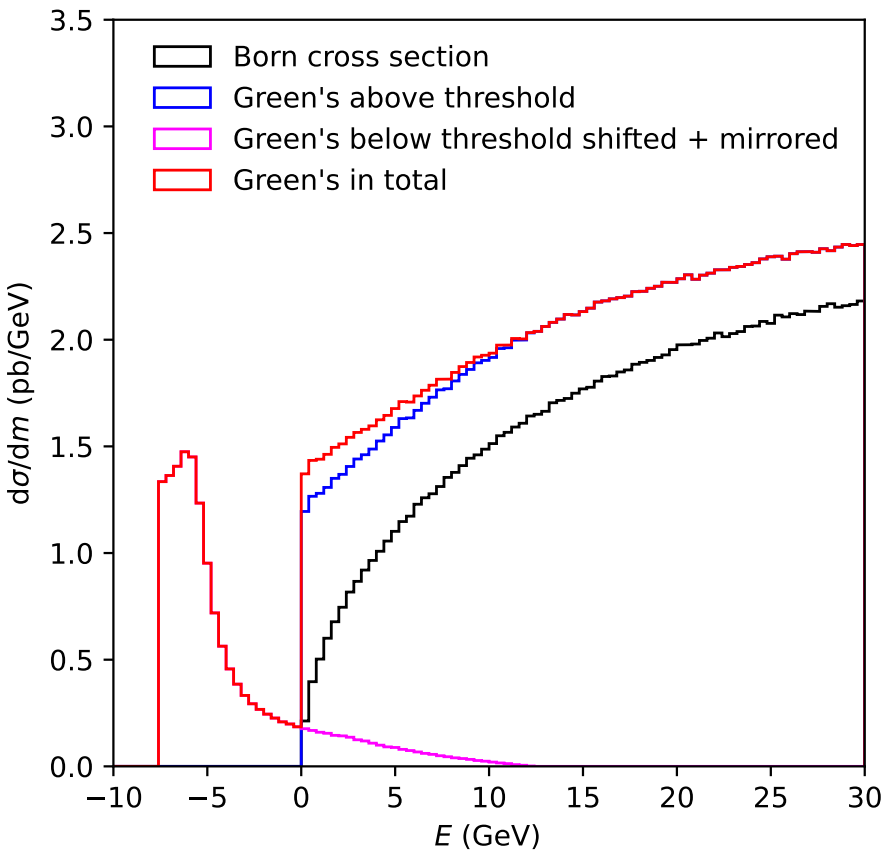

Full simulation pp at 13 TeV,
300 GeV $< \hat{m} <$ 400 GeV.
$\mathrm{gg} \to \mathrm{t\bar{t}}$ 2/7 singlet, 5/7 octet.
$\mathrm{q\bar{q}} \to \mathrm{t\bar{t}}$ all octet.

As above, but change
$m_\mathrm{t} = 172.5 \to 168.7$ GeV
for mirrored part,
so $\langle E \rangle = +3.82 \to -3.90$ GeV.

Advantages:
better $\langle \hat{m} \rangle$,
so better PDF weights;
good enough if $\Delta \hat{m} > \mathcal{O}(10\ \mathrm{GeV})$.

Disadvantages:
requires two sub-runs;
BW peak in wrong place,
also likely wrong β_t.

Backup: Old cross section comparison

Consider 13 TeV pp collisions in range $300 < \hat{m} < 400$ GeV:

	σ (pb)			change
initial state	gg	$\mathrm{q\bar{q}}$	sum	
Born	88.5	18.7	107.2	—
Coulomb	108.1	16.9	125.0	+16.5%
Green's, $E > 0$	108.3	17.1	125.4	—
Alt. 1, $E < 0$	5.30	0.40	5.70	+22.3%
Alt. 2, $E < 0$	5.86	0.41	6.27	+22.8%
Alt. 3, $E < 0$	6.29	0.47	6.76	+23.3%
all octet	1.93	0.47	2.40	−6.2%
all singlet	17.1	4.4	21.5	+121%

So alternative 3 maybe slightly higher $\sigma(E < 0)$ than warranted, but overall looks good as most realistic modelling.

Beware significant impact of colour factors,
which could be changed by higher-order effects.